Journal of Medicinal Chemistry Article

J. Med. Chem. **2010,** *53,* 8387–8399 **8387**
DOI: 10.1021/jm101092u

Non-Natural Macrocyclic Inhibitors of Histone Deacetylases: Design, Synthesis, and Activity†

Luciana Auzzas,[‡,§] Andreas Larsson,[‡,∥] Riccardo Matera,[‡] Annamaria Baraldi,[‡] Benoît Deschênes-Simard,[‡] Giuseppe Giannini,[⊥] Walter Cabri,*[,⊥] Gianfranco Battistuzzi,[⊥] Grazia Gallo,[⊥] Andrea Ciacci,[⊥] Loredana Vesci,[⊥] Claudio Pisano,[⊥] and Stephen Hanessian*[,‡]

[‡]*Department of Chemistry, Université de Montréal, P.O. Box 6128, Station Centre-ville, Montréal, QC, H3C 3J7 Canada,* [§]*Istituto di Chimica Biomolecolare, Consiglio Nazionale delle Ricerche, Traversa La Crucca 3, 07100 Sassari, Italy,* [∥]*Department of Chemistry, Umea University, 90187 Umea, Sweden, and* [⊥]*Sigma-Tau Research and Development, Via Pontina Km 30.400, 00040 Pomezia, Roma, Italy*

Received August 23, 2010

Nonpeptidic chiral macrocycles were designed on the basis of an analogue of suberoylanilide hydroxamic acid (**2**) (SAHA, vorinostat) and evaluated against 11 histone deacetylase (HDAC) isoforms. The identification of critical amino acid residues highly conserved in the cap region of HDACs guided the design of the suberoyl-based macrocycles, which were expected to bear a maximum common substructure required to target the whole HDAC panel. A nanomolar HDAC inhibitory profile was observed for several compounds, which was comparable, if not superior, to that of **2**. A promising cytotoxic activity was found for selected macrocycles against lung and colon cancer cell lines. Further elaboration of selected candidates led to compounds with an improved selectivity against HDAC6 over the other isozymes. Pair-fitting analysis was used to compare one of the best candidates with the natural tetrapeptide apicidin, in an effort to define a general pharmacophore that might be useful in the design of surrogates of peptidic macrocycles as potent and isoform-selective inhibitors.

Introduction

Epigenetic therapy with agents targeting heritable changes in gene expression that do not involve alteration in the DNA sequences is a new and rapidly developing area in pharmacology.[1] Together with DNA methylation and RNA-associated silencing, important post-translational modifications such as the ones controlled by histone acetyltransferases (HATs)[a] and histone deacetylases (HDACs) are among the most studied epigenetic mechanisms. By means of a delicate balance of competing activities, HATs and HDACs control the acetylation status of highly conserved lysine residues of histone proteins, changing the accessibility of transcription factors to DNA and thereby affecting the chromatin remodeling process. Perturbations of this balance have been linked to cancer, and inhibition of HDACs has been shown to have an antiproliferative effect on tumor cell lines, resulting in a considerable interest in this field.[2] In addition, an increasing number of non-histone proteins whose activity is finely tuned upon lysine modification are being identified, expanding the role and pharmacological potential of acetylation in human cells.[2,3]

Among HDAC enzymes, 11 isoforms are known to belong to the group of zinc-dependent metalloproteins[4] and fall into structurally and functionally different classes (class I, II, and IV HDACs).[5] The majority of HDAC inhibitors affect all the isoforms with equivalent potency. To date, little is known about the function and expression for each HDAC class and, in particular, about the structural origin of selectivity for the design of class- and/or isoform-selective HDAC inhibitors.[6−8] Furthermore, a complete HDAC inhibitory profiling is often not available, because the development of effective isozyme-based assays is relatively recent and not yet a common practice.[6c−e,9] Only a few isozyme and class-selective HDAC inhibitors have been developed recently[10] and are undergoing clinical trials to assess the benefit of selectivity on potency.[6a−e] Until further evidence becomes available, promiscuous HDAC inhibitors are still considered superior and safer than class I-selective agents, because they inhibit important class II HDAC isoforms playing a strategic role in cancer therapy, such as HDAC6, without exhibiting an increased toxicity.[6a−e,9b] In this regard, information highlighting specific isoforms as potential anticancer targets is continuously becoming available,[6a−e] calling for the design and synthesis of new selective inhibitors.

The list of known inhibitors of class I and II HDACs covers a wide cross section of structures,[2] including simple natural products such as trichostatin A (**1**, TSA),[11] their unnatural surrogates such as suberoylanilide hydroxamic acid (**2**) (SAHA, vorinostat),[12] and complex macrocyclic natural compounds such as trapoxin B (**3**), apicidin A (**4**), and the recently launched depsipeptide **6** (FK288, romidepsin) (Figure 1).[13]

†Protein Data Bank entries 1T67, 2V5X, and 3C10.

*To whom correspondence should be addressed. S.H.: phone, (514) 343-6738; fax, (514) 343-5728; e-mail, stephen.hanessian@umontreal.ca. W.C.: phone, +39-06-9139-4441; fax, +39-06-9139-3638; e-mail, walter.cabri@sigma-tau.it.

[a] Abbreviations: HDAC(s), histone deacetylase(s); HATs, histone acetyltransferases; TSA, trichostatin A; SAHA, suberoylanilide hydroxamic acid; DPPA, diphenyl phosphoryl azide; DEAD, diethyl azodicarboxylate; DIAD, diisopropyl azodicarboxylate; DIBALH, diisopropylaluminum hydride; PDC, pyridinium dichromate; EDC, *N*-ethyl-*N*′-(3-dimethylaminopropyl)carbodiimide; DIPEA, diisopropylethylamine; HOBt, 1-hydroxybenzotriazole; DEBPT, 3-(diethoxyphosphoryloxy)-1,2,3-benzotriazin-4(3*H*)-one; SRB, sulforhodamine B; DBU, 1,8-diazabicyclo[5.4.0]undec-7-ene; Pip, D-pipecolic acid; Aoda, 2-amino-8-oxodecanoic acid; FCS, fetal calf serum; OPLS, optimized potentials for liquid simulations; PRCG, Polak−Ribiere Conjugate Gradient; TNCG, Truncated Newton Conjugate Gradient; rmsd, root-mean-square deviation; PDB, Protein Data Bank.

Published on Web 11/12/2010

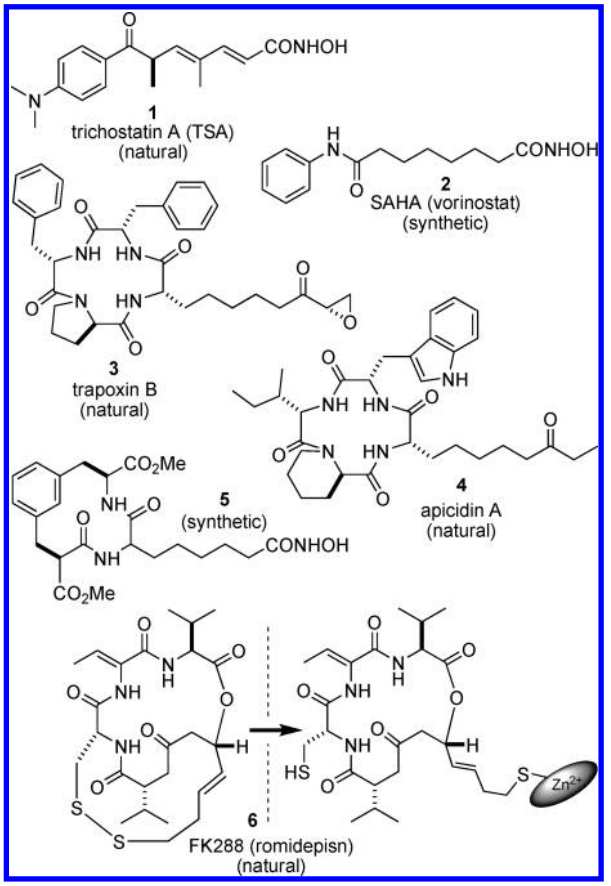

Figure 1. Structures of natural and unnatural HDAC inhibitors.

Typically, HDAC inhibitors are substrate mimics of the linear acetyl lysine side chain with a zinc-binding group replacing the scissile acetamide bond and a "cap" motif that binds the rim outside the active site of the enzyme.[7,8] The most effective inhibitors feature a hydroxamic acid group as the zinc-binding motif,[14] although a significant cap interaction with large peptide-based macrocycles often leads to a high activity even in the presence of mild binding groups, resulting in an overall potency superior to that of **2**.[15] Moreover, as the rim is divergent among the different HDAC isoforms,[16] cyclic peptides have the potential to discriminate among them.[13] Various analogues of natural cyclic peptides retaining the activity of the parent natural products have been synthesized, providing some insights into the structural requirements for achieving high activity and, in principle, selectivity.[15,17] For instance, Ghadiri and co-workers[17a,b] defined the pharmacophoric features required to modulate the HDAC activity of cyclic tetrapeptides inspired by the structure of apicidin **4**. Common geometrical requirements were found within a library of cyclic $\alpha_3\beta$ and $\alpha_2\beta_2$ peptides, which were used for the design of isoform-selective inhibitors based on peptidic architectures.

Nonpeptidic macrocycles represent an unexplored alternative to cyclic peptides.[18] By judicious design, they might offer simplified tools for probing the cap region of HDACs, in view of the design of analogues with increased potency and, possibly, selectivity. However, examples of designed unnatural macrocycles with HDAC activity, such as the synthetic compound **5** depicted in Figure 1, are somewhat scarce.[19]

Recently, we showed that the ω-benzyloxy-substituted suberoyl-based hydroxamic acid **7** (Scheme 1) is an inhibitor

Scheme 1. Structures of Lead Compound **7**, Proposed Macrocyclic Prototype **A**, and Its Assembly

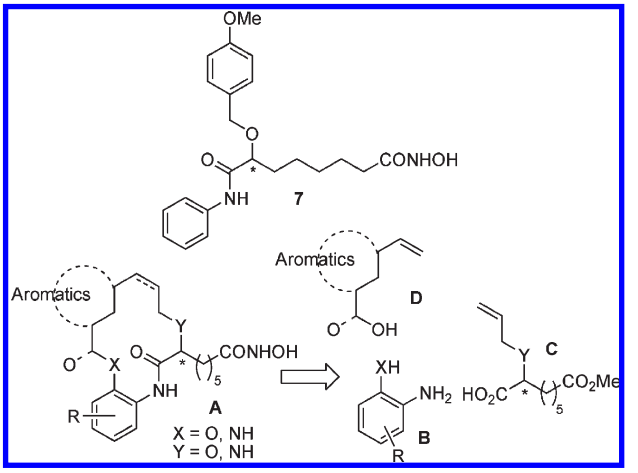

comparable to **2** against HDAC1−11, and a better antiproliferative agent than **2** against three different human cancer cell lines (NB4, H460, and HCT-116).[20] No significant difference in inhibitory activity was found between the racemic **7** and its individual enantiomers against zinc-dependent HDACs, and this equivalence found support in modeling of the individual enantiomers of **7** in the crystal structure of either HDAC8[7a−c] or HDAC7.[7d] Two highly conserved Phe residues are present in the rim outside HDAC catalytic sites[7c,h] (Phe152 and Phe208 in HDAC8), in opposite orientations, which were found to ensure favorable $\pi-\pi$ interactions with one aromatic ring or the other (anilido and *p*-methoxybenzyl ring) of each enantiomer of **7**.[21] We reasoned that this property might be exploited for the design of constrained analogues of **7**, which could be recognized by the enzyme regardless of their chirality.[22] Considering the high level of conservation of Phe and Asp residues among the HDAC isoforms (Phe152, Phe208, and D101 in HDAC8),[7a,c,h,23] these novel macrocycles are expected, at least in principle, to bear pharmacophoric determinants close to a maximum common substructural consensus required to target the whole HDAC panel, provided that the strong zinc-binding group hydroxamic acid is used.[15,22]

Results and Discussion

Simple macrocyclic variants of **2** and **7** were first designed, according to general structure **A** (Scheme 1).[24] A lipophilic linker was chosen to force the branching point at the α-position of the suberic acid chain in a spatially constrained template. A small library of macrocycles that can be crafted by the combination of building blocks **B**−**D** were designed to be sequentially assembled by a phenolic Mitsunobu reaction or an amide coupling, followed by the formation of the anilide bond, and a macrocyclization using a ring closing metathesis reaction (Scheme 1).

To assess the influence of macrocycle size, we chose a simple aliphatic linker of various lengths as in racemic compounds (*R*/*S*)-**8a**−**c** (Figure 2). Aromatic tethers embedding a methoxy-substituted benzyloxy motif as in **7** were hence selected to be introduced into 14-member macrocycles [compounds **9** and **10** (Figure 2)]. Enantiopure **9** and **10** were also prepared to be compared to their racemic counterparts.

The synthesis commenced with the preparation of α-allyloxy acid building block **C** (Scheme 1). A common intermediate was envisaged, (*S*)- or (*R*)-**11**, which readily ensured the

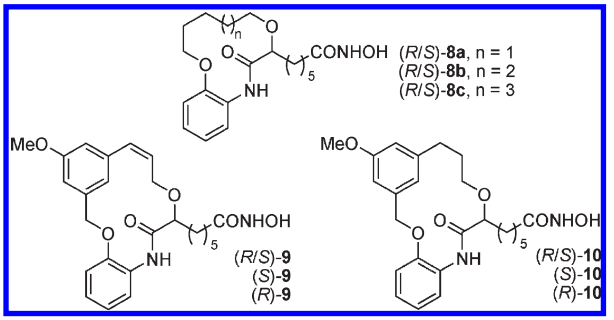

Figure 2. Macrocyclic hydroxamic acids **8**−**10**.

Scheme 2. Synthesis of *O*-Allyloxy Acid (*S*)- and (*R*)-**14** and *N*-Allylamino Acid (*S*)-**18**

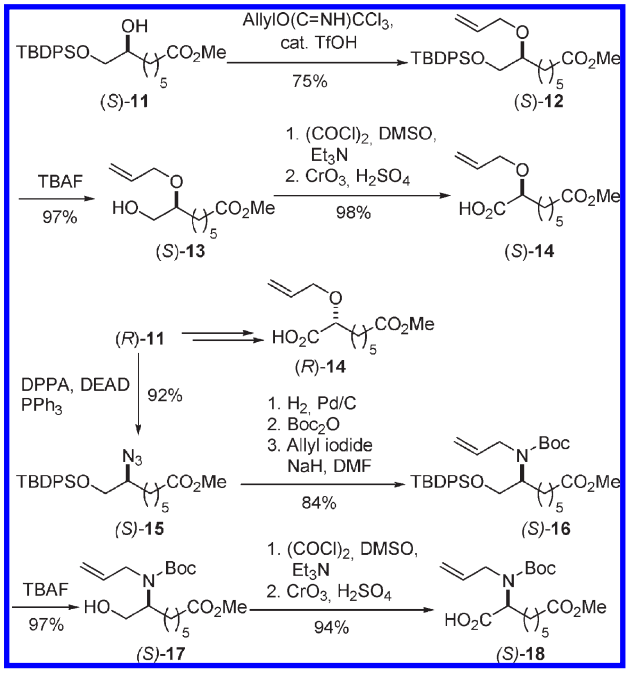

preparation of both enantiomers of **14** as well as the *S*-configured aza analogue **18** (Scheme 2). *O*-Allylation of (*S*)-**11**[20a] with allyl trichloroacetimidate led to (*S*)-**12**, which was desilylated to give (*S*)-**13**. Oxidation to an aldehyde intermediate under Swern conditions followed by Jones oxidation gave carboxylic acid (*S*)-**14** almost quantitatively. In parallel, (*R*)-**14** was obtained starting from the corresponding enantiomer (*R*)-**11**.[20]

In a divergent path, intermediate (*R*)-**11** also served for the synthesis of amino acid (*S*)-**18**. Azidation with inversion of configuration was performed under conventional Mitsunobu conditions[25] and led to (*S*)-**15** in 92% yield. Hydrogenation under Pd/C catalysis followed by *N*-Boc protection on the crude resulting amine gave the protected ester intermediate, which was smoothly *N*-allylated under standard conditions (NaH, allyl iodide at 0 °C) to give (*S*)-**16**. In parallel with the same sequence described for the *O*-allyl ether analogue (*S*)-**12**, the *N*-Boc-protected allylamino acid (*S*)-**18** was obtained in 91% yield starting from (*S*)-**16**.

2-Alkenyloxy anilines **21b,c**[26] required for assembling macrocycles (*R*/*S*)-**8b,c** (Figure 2) were efficiently prepared via a phenolic Mitsunobu reaction between *o*-nitrophenol **19** and the proper terminal alkenol, followed by reduction of the resulting nitro derivatives **20b,c** with $SnCl_2 \cdot 2H_2O$ (Scheme 3).

Scheme 3. Synthesis of Anilines **21b,c** and **26**

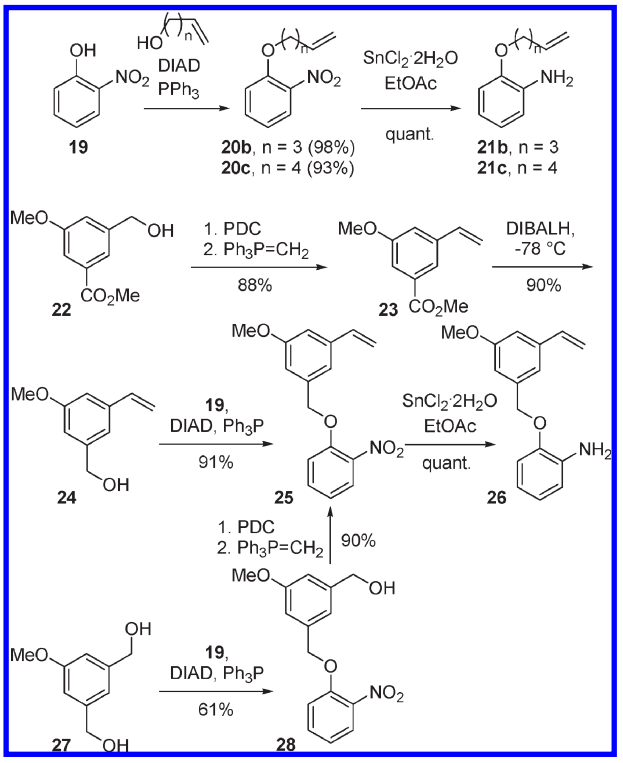

Scheme 4. Synthesis of Macrocycles (*R*/*S*)-**8a**−**c**

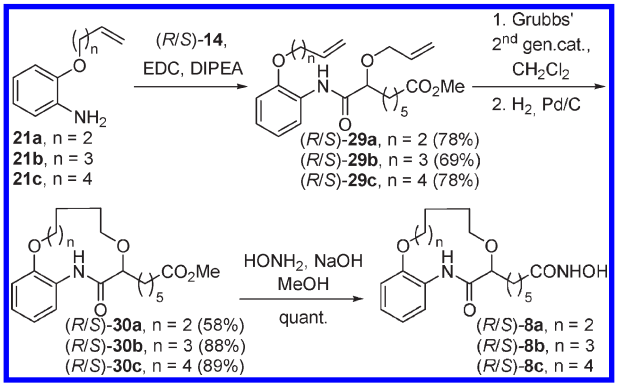

2-Benzyloxy aniline **26** required for macrocycles **9** and **10** (Figure 2) was prepared by reaction of *o*-nitrophenol **19** with benzyl alcohol **24** in the presence of diisopropyl azodicarboxylate (DIAD) and PPh_3, and subsequent reduction of the nitro derivative **25** with $SnCl_2 \cdot 2H_2O$ in quantitative yield (Scheme 3). Intermediate **24** could be efficiently prepared by a diisobutylaluminum hydride (DIBALH) reduction of the corresponding methyl ester **23**, in turn easily obtained from **22**[27] by pyridinium dichromate (PDC) oxidation to an aldehyde intermediate, followed by a Wittig methylenation (79% yield for three steps). Alternatively, stryrene derivative **25** could be prepared by desymmetrization of the known benzyl alcohol **27**[28] via a Mitsunobu reaction and a subsequent two-step vinylation of **28**.

Macrocycles (*R*/*S*)-**8a**−**c** were assembled as shown in Scheme 4. A coupling reaction between racemic carboxylic acid **14** and anilines **21a**−**c** mediated by *N*-ethyl-*N*′-(3-dimethylaminopropyl)carbodiimide (EDC) led to the corresponding anilides (*R*/*S*)-**29a**−**c** in yields ranging from 69 to 78%. The ring closing metathesis reaction[29] promoted by

Scheme 5. Synthesis of Macrocycles **9** and **10**[a]

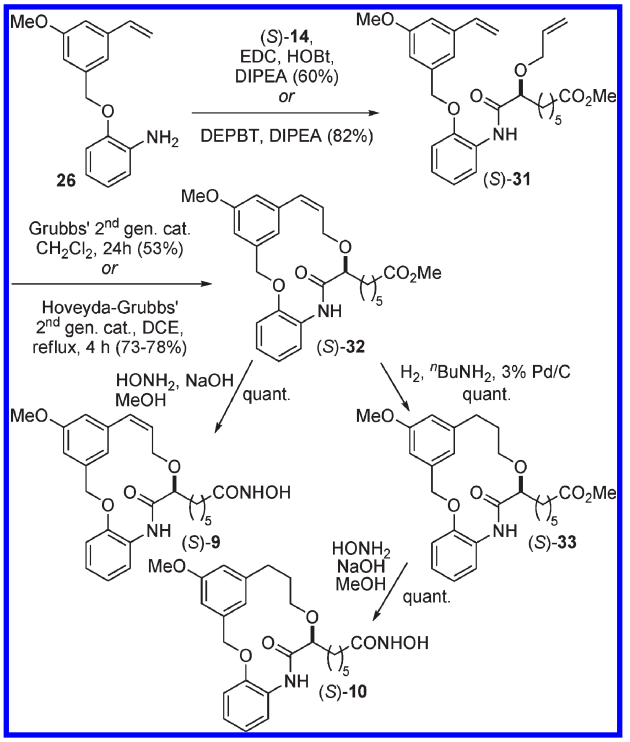

[a] Only the *S*-isomer is shown.

Grubbs' second-generation catalyst[30] in CH_2Cl_2 proceeded smoothly, leading to the intermediate macrocyclic olefins as a mixture of *E* and *Z* isomers in good to excellent yield (72−99%). After reduction of the double bond under H_2 and Pd/C, the resulting methyl esters (*R*/*S*)-**30a**−**c** were quantitatively converted to the desired hydroxamic acids (*R*/*S*)-**8a**−**c** by reaction with $HONH_2$ in MeOH in the presence of aqueous NaOH.

In preliminary trials, coupling of (*S*)-**14** with aniline **26** with EDC in the presence of 1-hydroxybenzotriazole (HOBt) and diisopropylethylamine (DIPEA) led to anilide **31**, albeit in a moderate yield [60% (Scheme 5)]. The same reaction promoted by Goodman's reagent [(3-diethoxyphosphoryloxy)-1,2,3-benzotriazin-4(3*H*)-one (DEPBT)][31] in the presence of DIPEA proved to be more efficient and was used for anilides (*S*)- and (*R*)-**31** (82% yield). Ring closing metathesis in the presence of Grubbs' second-generation catalyst in CH_2Cl_2 produced the desired macrocycles (*S*)- and (*R*)-**32** in 24−48 h, but only in a moderate yield (53%), along with homocoupling side products and unreacted starting material. After optimization, we found that using the Hoveyda−Grubbs' second-generation catalyst[32] in refluxing dichloroethane (DCE), the desired macrocycle could be efficiently obtained in only 2 h in 73−78% average yield. Both conditions provided the unsaturated macrocycle **32** as a sole *Z* isomer. This configuration was substantiated by the observation of a coupling constant of 11.2 MHz in the ^{1}H NMR analysis and confirmed by X-ray analysis of (*S*)-**32** (Figure 3). With both the enantiomers of the unsaturated macrocycle **32** in hand, the (*S*)-, (*R*)-, and (*R*/*S*)-**9** hydroxamates were prepared through the previously described protocol ($HONH_2$, aqueous NaOH in MeOH). Alternatively, after reduction of the double bond (H_2, Pd/C, ^{n}BuNH$_2$)[33] to racemic and enantiopure **33**, macrocyclic hydroxamic acids (*S*)-, (*R*)-, and (*R*/*S*)-**10** could be obtained.

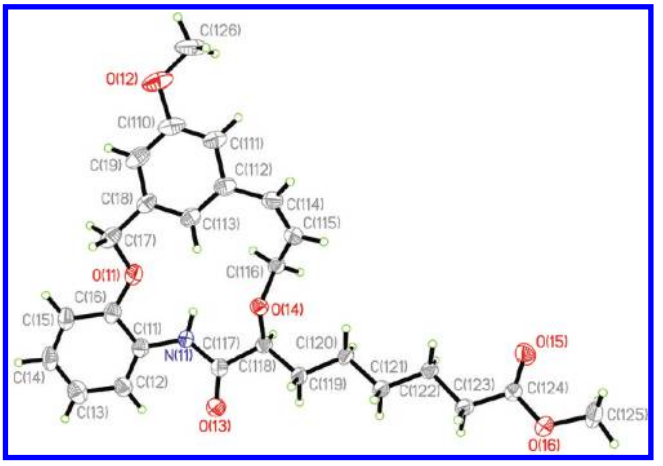

Figure 3. ORTEP view of (*S*)-**32**.

The HDAC inhibitory profile of macrocyclic hydroxamic acids **8**−**10** was investigated by measuring their potency in inhibiting 11 isolated human HDAC isozymes in the presence of a fluorogenic peptide bound to the RHKK(Ac) fragment of p53 (residues 379−392) as the substrate, and using **1**,[11] **2**,[12] and dacinostat (NVP-LAQ824)[34] as the reference compounds (Table 1).[20,24,35] Furthermore, their antiproliferative activity on two human tumor cell lines (H460 and HCT-116) was also evaluated (Table 2).

Macrocyclic compounds embedding an aliphatic linker [compounds (*R*/*S*)-**8a**−**c**] showed an HDAC inhibitory profile comparable to that of **2**, albeit inferior to that of acyclic reference compound (*R*/*S*)-**7**. Within this series, an improvement in activity proportional with the increase in macrocycle size and flexibility was observed. The 14-member ring macrocycle (*R*/*S*)-**8c** exhibited an inhibitory activity in the low micromolar range against 10 HDACs (HDAC1−5 and 7−11) and nanomolar activity against HDAC6 (Table 1).

Macrocycles **9** and **10**, embedding an extra aromatic ring in the linker, displayed the highest activity, with a nanomolar inhibitory profile against all HDAC isoforms. Only a slight preference for the *S* isomer was observed for **9** against all HDACs [$IC_{50(S/R)}$ = 0.08−0.6]. The same preference was less evident between the two enantiomers of **10**. Compound (*S*)-**9** emerged as the best candidate, displaying a subnanomolar activity on HDAC6 (0.84 nM) comparable to that of **1** and activity 10-fold higher than that of dacinostat.

Reduction of the double bond of (*S*)-**9** as in (*S*)-**10** did not appreciably affect the overall HDAC inhibitory profile [average $IC_{50(unsat/sat)}$ = 0.5]. The same relationship could be found also in the racemic and enatiomeric counterparts (*R*)-**9** and (*R*)-**10**.

Although the HDAC profile suggested a pan-inhibitory activity, some preference for the inhibition of HDAC6 was observed for all the tested compounds [$IC_{50(HDAC6/HDAC2)}$ = 0.003−0.02].

A promising cytotoxic activity was found for all the macrocycles against lung and colon cancer cell lines [H460 and HCT-116 human cell lines, respectively (Table 2)], which was comparable or even superior to that of **2**. No difference in cytotoxicity was detected between the two enantiomers of **9** or between macrocycles **9** and **10**.

To rationalize the biological results and potentially reveal how to increase the activity, we modeled the macrocycles into the active site of HDAC8 using a flexible ligand/rigid receptor docking method (see the Experimental Section). Docking

Table 1. In Vitro Inhibitory Activity (IC_{50}) of Macrocycles **8**−**10** against Isoforms HDAC1−11[a]

	class I				class IIa				class IIb		class IV
	HDAC1	HDAC2	HDAC3	HDAC8	HDAC4	HDAC5	HDAC7	HDAC9	HDCA6	HDAC10	HDAC11
1	7.12	22.95	10.32	89.53	12.07	16.48	22.46	38.12	0.42	20.10	15.15
2	258.00	921.00	350.00	243.00	493.00	378.00	344.00	316.00	28.60	456.00	362.00
dacinostat	3.23	15.70	10.50	3.84	5.82	5.58	6.11	8.24	5.93	8.41	5.58
(*R*/*S*)-**7**	53.40	254.00	131.00	331.00	648.00	134.00	432.00	247.00	20.10	179.00	197.00
(*R*/*S*)-**8a**	949.00	1930.00	369.00	643.00	2580.00	1340.00	1720.00	1900.00	15.60	1530.00	1210.00
(*R*/*S*)-**8b**	560.00	1570.00	176.00	1100.00	1200.00	878.00	738.00	687.00	10.10	683.00	564.00
(*R*/*S*)-**8c**	439.00	1540.00	240.00	286.00	1250.00	695.00	764.00	1040.00	9.38	958.00	546.00
(*R*/*S*)-**9**	30.70	207.00	39.60	119.00	159.00	55.40	72.60	99.60	1.97	70.70	57.70
(*S*)-**9**	31.70	158.00	55.70	198.00	79.40	62.20	27.80	60.60	0.84	62.50	22.90
(*R*)-**9**	78.10	382.00	89.00	206.00	284.00	155.00	180.00	302.00	10.20	152.00	97.10
(*R*/*S*)-**10**	204.00	793.00	246.00	444.00	447.00	341.00	279.00	336.00	8.44	320.00	226.00
(*S*)-**10**	72.20	268.00	93.60	136.00	118.00	109.00	61.20	123.00	3.43	190.00	103.00
(*R*)-**10**	102.00	425.00	94.50	90.70	454.00	150.00	271.00	322.00	3.92	200.00	174.00

[a] Values are the means of a minimum of three experiments and are given in nanomolar. For further details, see the Experimental Section.

Table 2. In Vitro Cytotoxic Activity (IC_{50}) of Macrocycles **8**−**10**[a]

	H460 (lung)	HCT-116 (colon)
1	0.100	0.043
2	3.400	1.200
dacinostat	0.070	0.018
(*R*/*S*)-**7**	0.520	0.220
(*R*/*S*)-**8a**	2.000	0.690
(*R*/*S*)-**8b**	1.000	0.580
(*R*/*S*)-**8c**	0.620	0.350
(*R*/*S*)-**9**	0.880	0.450
(*S*)-**9**	1.050	0.690
(*R*)-**9**	0.820	0.640
(*R*/*S*)-**10**	0.870	0.690
(*S*)-**10**	0.740	0.520
(*R*)-**10**	0.680	0.850

[a] Values are the means of a minimum of three experiments and are given in micromolar. Growth inhibition was assessed by a sulforhodamine B (SRB) assay. For further details, see the Experimental Section.

analysis of HDAC8[7a−c] confirmed the adaptability of the designed macrocycles on the cap region of this isozyme. Among the macrocycles containing an aliphatic tether, the best contacts were found with the 14-member cycle (*R*/*S*)-**8c**. As expected, both *R* and *S* isomers were extruded from the enzyme cavity, forming a $\pi-\pi$ interaction with Phe152 and Phe208, respectively, albeit an interaction weaker than those observed with (*S*)- and (*R*)-**7**.[20a] Extra stabilization resulted from a H-bond interaction between their anilide bond and Asp101 (Figure SI1 of the Supporting Information).

Macrocycles **9** and **10** displayed comparable orientations and interactions with HDAC8, irrespective of the presence of the double bond (Figure 4; only (*S*)-**9** is shown). Although only weak interactions with both aromatic residues of **9** and **10** with Phe152 and Phe208 were observed in HDAC8, favorable contacts with Tyr100 and Lys33 further stabilized their binding.[21] Docking of *R* and *S* isomers of **9** in this isoform did not account for any difference in their binding, consistent with the results obtained in the enzymatic test on this isoform (Table 1) and with our prediction (Figure SI2 of the Supporting Information).[36]

Binding mode analysis of (*S*)-**9** and (*S*)-**10** in HDAC8 revealed the possibility of adding an extra contact point with the conserved Asp101 residue in the rim of this isozyme by appropriately introducing a H-donor group within the macrocycle (Figure 4). Bioisosteric replacement of the macrocyclic oxygen bridge of (*S*)-**9** with an amino function was expected to serve this purpose and prompted the synthesis of the aza

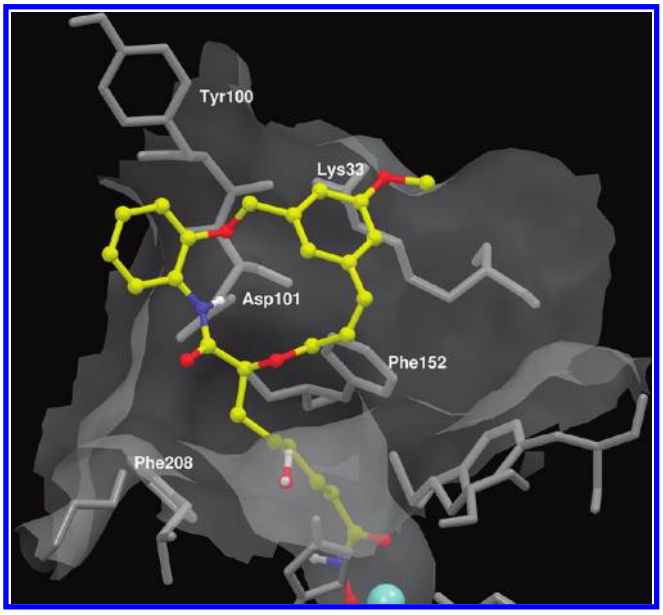

Figure 4. Predicted mode of binding of (*S*)-**9** in the HDAC8 crystal structure.

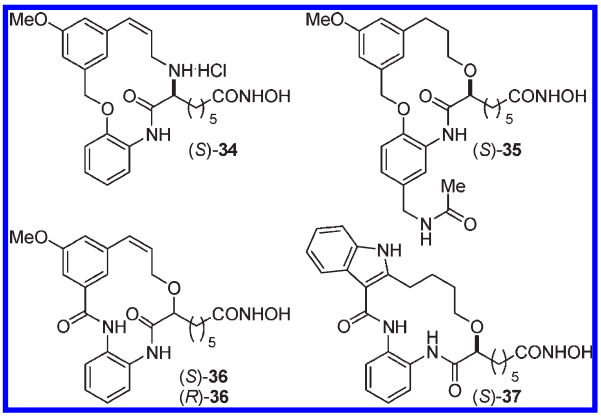

Figure 5. Macrocyclic hydroxamic acids **34**−**37**.

macrocycle (*S*)-**34** (Figure 5). Unexpectedly, a different orientation was observed in docking (*S*)-**34** in HDAC8 as compared to (*S*)-**9** (Figure 6), and a 30% decrease in the level of the main interactions seen for the parental compound was recorded. However, the complex gained stabilization through

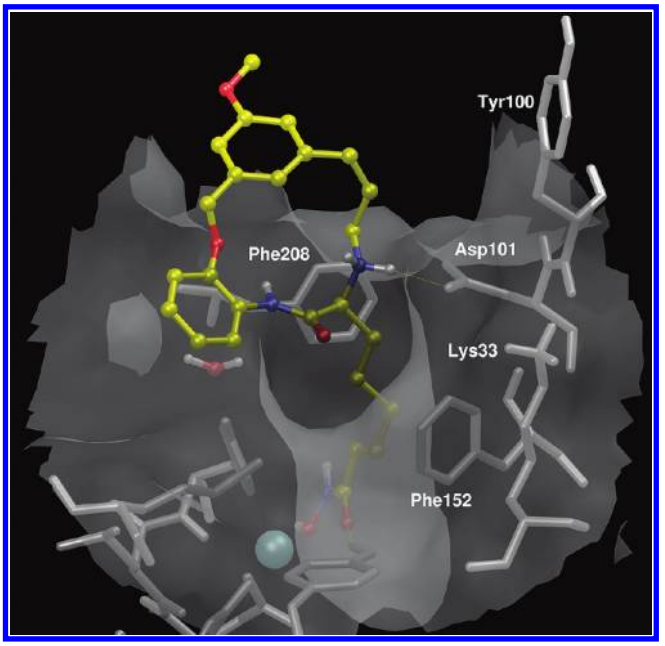

Figure 6. Best docking solution of (*S*)-**34** into the HDAC8 crystal structure.

Scheme 6. Synthesis of Macrocycle (*S*)-**34**

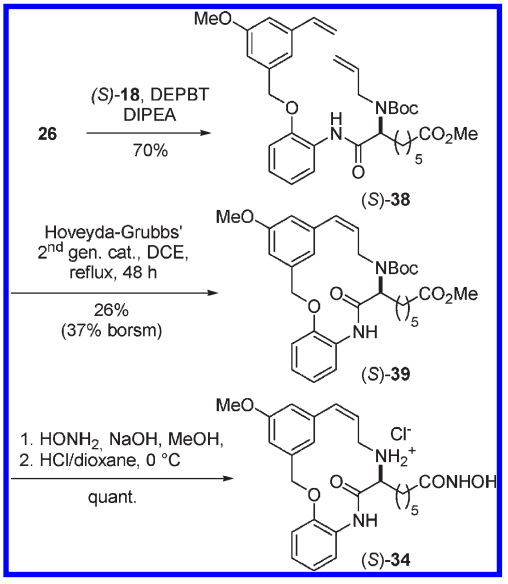

a salt bridge with Asp101.[37] The acetamido analogue (*S*)-**35** was also prepared (Figure 5).[38]

Furthermore, diamido isosteres of macrocycles **9**, as well as an indole-containing macrocycle, were envisaged as promising analogues [compounds (*R*)- and (*S*)-**36** and (*S*)-**37** (Figure 5)]. We hoped these macrocycles would benefit from enhanced interactions with the conserved Phe residues of HDACs (Phe152 and Phe208 in HDAC8) as compared to the parental compound **9** thanks to the additional CONH functionality, which was thought to offer extra stabilization by forming a H-bond with Asp101 (Figures SI4 and SI5 of the Supporting Information).[39]

Nitrogen-containing macrocycle (*S*)-**34** was synthesized analogously to its oxygenated counterpart **9** (Scheme 6). Unfortunately, anilide (*S*)-**38**, prepared by coupling aniline **26** with acid (*S*)-**18** in the presence of DEPBT, underwent the metathesis reaction to macrocyclic olefin (*S*)-**39** in only 26% isolated yield (37% borsm) with Hoveyda−Grubbs' second-generation catalyst in refluxing DCE for 48 h. An explanation for the sluggish reaction can be found in the considerable steric hindrance of the *N*-Boc-containing substrate (*S*)-**38** in comparison to the oxygenated counterpart **31**, for which the substantial formation of homocoupling side products and a significant decomposition of the starting material account.[40] Nevertheless, the desired (*S*)-**34** could be obtained in a quantitative yield by converting the methyl ester function in (*S*)-**39** to a hydroxamic acid intermediate and finally deblocking the *N*-Boc protection with HCl in dioxane.

Scheme 7. Synthesis of Aniline **44**

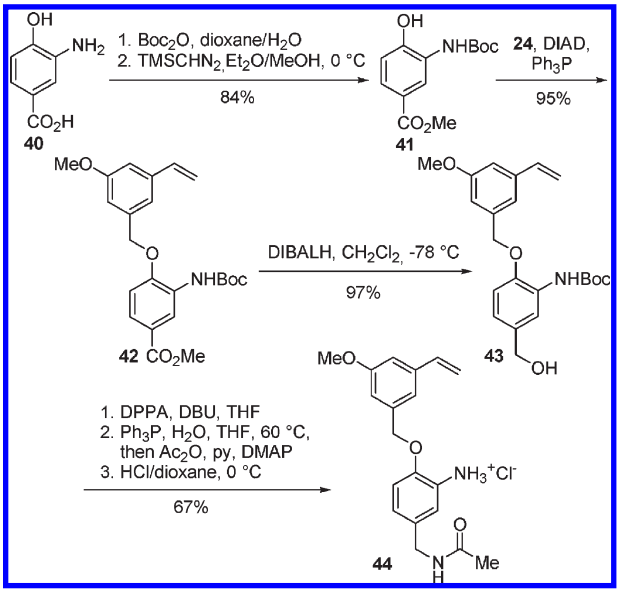

The synthesis of macrocycle (*S*)-**35** required the preparation of the aniline building block **44** (Scheme 7). After orthogonal protection of the commercially available aniline **40** by *N*-Boc protection and esterification as a methyl ester, phenol **41** was reacted under Mitsunobu conditions with benzyl alcohol **24**, leading to intermediate **42** in excellent yield (95%). After reduction of the methyl ester group of **42** to benzyl alcohol **43** with DIBALH, a straightforward four-step sequence was used to install the acetamido group, which consisted of (i) azide formation under Thomson's condition[41] and (ii) Staudinger reaction,[42] followed by (iii) acetylation of the resulting amine and (iv) final removal of the *N*-Boc protection. From this sequence, aniline **44** was obtained in 67% yield overall.

Coupling product (*S*)-**45**, smoothly obtained by reaction of aniline **44** and carboxylic acid (*S*)-**14** in the presence of DEPBT (Scheme 8), was cyclized under the same condition described for anilide **31** (Hoveyda−Grubbs' second-generation catalyst in DCE at reflux temperature) and led to (*S*)-**46** as a sole *Z* isomer in moderate yield (55%). The presence of the acetamido group in (*S*)-**45**, which may coordinate the ruthenium center in the catalyst, and the difficulty in isolating (*S*)-**46** because of its high polarity might explain the reasons for the low recovery after the metathesis reaction. After reduction of the double bond (H_2, Pd/C, ^{n}BuNH$_2$),[33] direct conversion of the methyl ester function in (*S*)-**47** to hydroxamic acid afforded (*S*)-**35** in quantitative yield in two steps.

In parallel with the general Scheme 1, diamide-containing macrocycles (*R*)- and (*S*)-**36** and **37** were prepared by combining allyloxy acid (*R*)-**14** and/or (*S*)-**14** with the appropriate aniline building blocks **52** and **59** (Scheme 9, only the *S*

Scheme 8. Synthesis of Hydroxamic Acid (*S*)-**35**

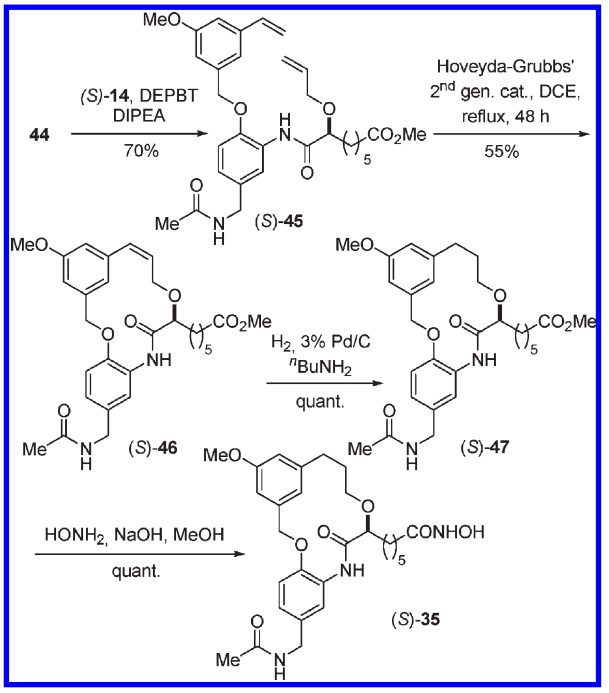

Scheme 9. Synthesis of Macrocycles (*S*)- and (*R*)-**36**[a]

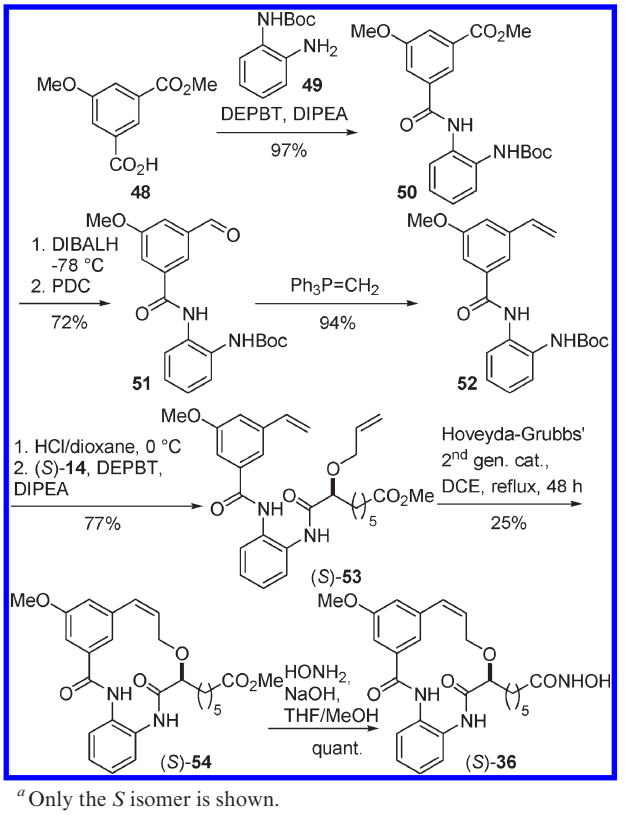

[a] Only the *S* isomer is shown.

isomer is shown; Scheme 10). Coupling of the orthogonally protected aniline **49**[43] with the known benzoic acid **48**[27] in the presence of DEPBT gave anilide **50** in 97% yield. Upon reduction of the methyl ester group with DIBALH, vinylation was performed as previously described in 87% yield for two steps. Following the acid-mediated *N*-Boc deprotection of **52** to the aniline intermediate, coupling with acids (*R*)- and (*S*)-**14** was performed using the usual protocol and led to diamide

Scheme 10. Synthesis of Macrocycle (*S*)-**37**

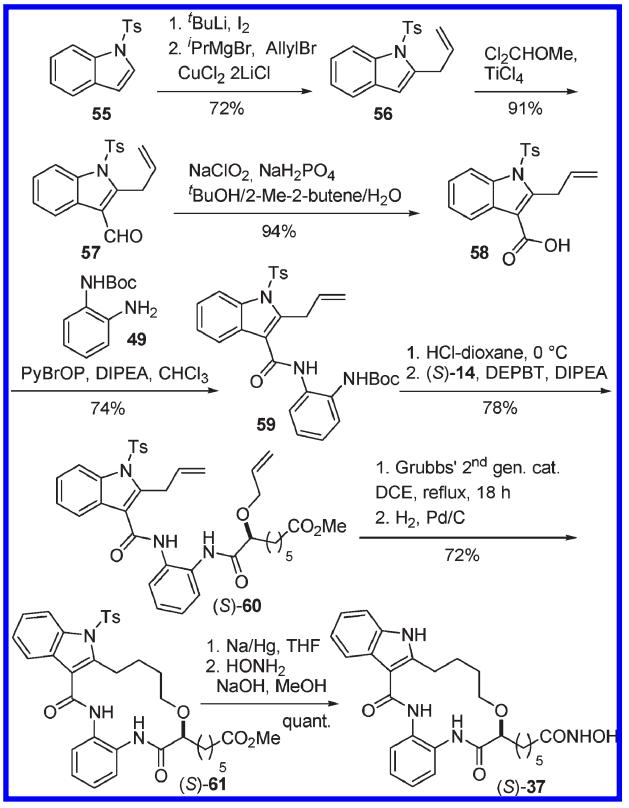

(*R*)- and (*S*)-**53** in 77% yield. Ring closing metathesis in the presence of 10 mol % Hoveyda-Grubbs' second-generation catalyst afforded macrocycle (*R*)- and (*S*)-**54** after refluxing for 2 days in DCE (25% yield).[44] The usual treatment of methyl esters (*R*)- and (*S*)-**54** with $HONH_2$ in aqueous NaOH, MeOH, and THF afforded the desired hydroxamic acids (*R*)- and (*S*)-**36**.

Indole-containing macrocycle (*S*)-**37** was prepared in an analogous way (Scheme 10). Carboxylic acid **58** was chosen as the precursor for the preparation of the requisite aniline **59**. Conversion of *N*-tosyl indole **55** to 2-allyl indole **56** was performed following conventional methods.[45] After $TiCl_4$-promoted formylation,[46] aldehyde **57** was smoothly converted to carboxylic acid **58** and coupled with phenylendiamine **49** (70% yield for two steps). The resulting *N*-Boc-protected aniline **59** was quantitatively converted to the aniline hydrochloride salt intermediate, which was used without further purification for the subsequent coupling reaction with acid (*S*)-**14**. Diamide (*S*)-**60** was obtained in good yield under conventional Goodman's conditions. After cyclization to the olefin intermediate in the presence of Grubbs' second-generation catalyst, and reduction of the olefin intermediate with H_2 and Pd/C to macrocycle (*S*)-**61**, *N*-detosylation was achieved in the presence of a Na/Hg alloy in THF.[47] Final conversion to the desired hydroxamic acid (*S*)-**37** was performed in the conventional way.

The biological activity of macrocyclic hydroxamic acids **34**−**37** is reported in Tables 3 and 4. In general, a good inhibitory profile was observed with close analogues of macrocycles **9** and **10**. The replacement of the oxygen at the α-position of the suberoyl chain of (*S*)-**9** with a nitrogen atom, as in (*S*)-**34**, did not appreciably modify the overall activity. The main difference was observed on HDAC8, whose level of inhibition was 5-fold higher with (*S*)-**34** than with (*S*)-**9**.

Table 3. In Vitro Inhibitory Activity (IC_{50}) of Macrocycles **34**−**37** against Isoforms HDAC1−11[a]

	class I				class IIa				class IIb		class IV
	HDAC1	HDAC2	HDAC3	HDAC8	HDAC4	HDAC5	HDAC7	HDAC9	HDCA6	HDAC10	HDAC11
2	258.00	921.00	350.00	243.00	493.00	378.00	344.00	316.00	28.60	456.00	362.00
(*S*)-**9**	31.70	158.00	55.70	198.00	79.40	62.20	27.80	60.60	0.84	62.50	22.90
(*S*)-**34**	27.70	171.00	15.80	39.30	52.10	24.70	15.90	22.60	0.75	46.50	34.80
(*S*)-**35**	41.30	128.00	63.10	45.40	64.80	65.20	34.30	47.70	0.40	65.10	45.90
(*S*)-**36**	864.00	3280.00	1114.00	534.00	5333.00	1660.00	4300.00	2020.00	59.00	2290.00	948.00
(*R*)-**36**	1340.00	2530.00	885.00	682.00	3480.00	1340.00	2070.00	1140.00	75.00	1880.00	1110.00
(*S*)-**37**	245.00	584.00	331.00	297.00	1690.00	496.00	2230.00	602.00	4.40	627.00	379.00

[a] Values are the means of a minimum of three experiments and are given in nanomolar. For further details, see the Experimental Section.

Table 4. In Vitro Cytotoxic Activity (IC_{50}) of Macrocycles **34** and **35**[a]

	H460 (lung)	HCT-116 (colon)
2	3.400	1.200
(*S*)-**9**	1.050	0.690
(*S*)-**34**	0.510	0.400
(*S*)-**35**	6.800	3.740

[a] Values are the means of a minimum of three experiments and are given in micromolar. Growth inhibition was assessed via the SRB assay. For further details, see the Experimental Section.

The introduction of an acetamido group onto the anilide ring of (*S*)-**10**, as in (*S*)-**35**, produced a moderate increase in inhibitory activity. As expected, (*S*)-**34** and (*S*)-**35** exhibited a pan-inhibitory activity, with a subnanomolar activity against HDAC6 comparable to that of **1** and an activity 10-fold higher than that of dacinostat.

Although the diamide-based macrocycles **36** and **37** exhibited an overall decrease in activity, a notable selectivity toward HDAC6 was observed (10−500-fold over the other HDACs) (Table 3). This preference might be explained by the presence of a hydrophobic region composed of several aromatic residues surrounding the Phe566 residue in the rim of the HDAC6 channel (Tyr100 in HDAC8), which might accommodate the phenyl and indole rings of these relatively rigid macrocycles.[10c,48]

The cytotoxic activity of macrocycle (*S*)-**34** against lung and colon cancer cell lines [H460 and HCT-116 human cell lines, respectively (Table 4)] was higher than that of **2**. On the other hand, the acetamido group-containing (*S*)-**35** exhibited a lower activity.

Overall, only the aza analogue (*S*)-**34** emerged as a candidate as good as its oxygenated counterpart.

Despite their rigid structural arrangement and the presence of a stereogenic center, macrocycles **9** and **34**−**37** embed critical determinants opportunely placed for the indiscriminate binding of each of the 11 HDACs through highly conserved residues in their cap region. With the objective being an improved understanding of the properties of these macrocycles, a ligand-based study considering their superimposition to a known, selective inhibitor was performed, aiming at the individualization of overlaid conformations displaying a maximum geometrical overlap of relevant chemical features, such as H-bond donors and acceptors, hydrophobic groups, etc. Hence, a pair-fitting analysis was performed by the rigid alignment of each enantiomer of **9** with a prototypical natural tetrapeptide, apicidin A (**4**), a well-known class I HDAC inhibitor (Figure 1).[13b,49,50] We speculated that, despite the structural diversity between our synthetic macrocycles (*S*)- and (*R*)-**9** and **4**, minimal but strategic contact points could be revealed, possibly opening the way for the definition of a simplified pan-HDAC inhibitory model.

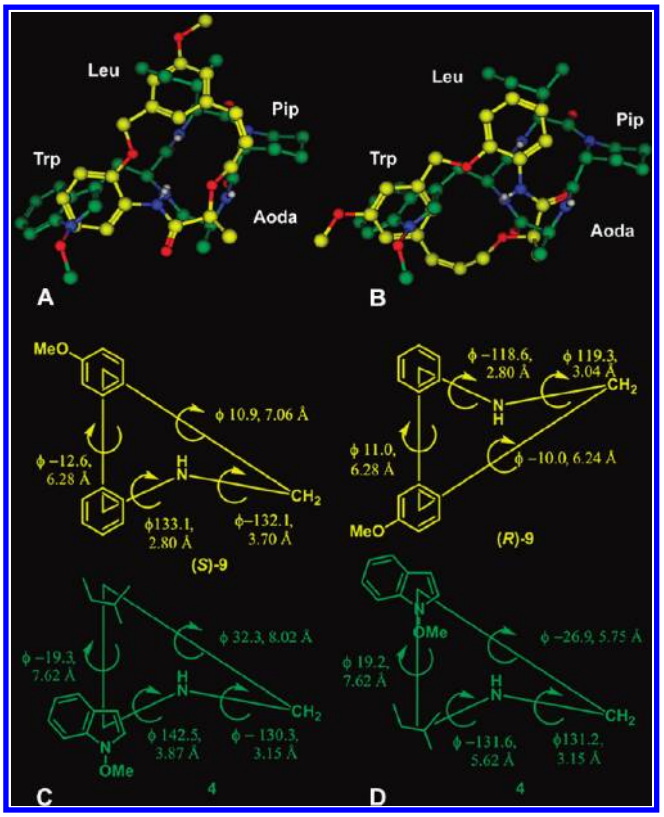

Figure 7. (A) Rigid alignment of the crystal structure of (*S*)-**9** (yellow) and apicidin A (**4**) (green). (B) Rigid alignment of the crystal structure of (*R*)-**9** (yellow) and **4** (green). (C) Two-dimensional (2D) model based on the structure of (*S*)-**9** (yellow) and **4** (green). (D) 2D model based on the structure of (*R*)-**9** (yellow) and **4** (green). In panels C and D, dihedral angles (ϕ) and distances between key determinants (angstroms) are given. Apicidin A (**4**) is shown as a *cis-trans-trans-trans* conformer,[49] consistent with recent findings by Ghadiri and co-workers.[50] Pip denotes D-pipecolic acid. Aoda denotes a 2-amino-8-oxodecanoic acid residue. Only the first methylene was considered in the pair-fitting analysis. Details of the calculation are available in the Experimental Section.

Several observations emerged from the superimposition of each enantiomer of **9** on the crystal structure of **4** (Figure 7).[49,50] A good overlapping was revealed between the expected key determinants in the *S* and *R* enantiomers of **9** and segments of apicidin A (**4**). In the rigid alignment of (*S*)-**9** and **4** (Figure 7A,C), the suberic aliphatic chains pointed in the same direction, albeit with a different angle. The aniline ring overlaid on the indole five-member ring of **4**, while the methoxyphenyl ring of (*S*)-**9** covered the region occupied by the Leu side chain. The amide bonds between suberic acid and aniline in (*S*)-**9**, and between suberic acid and Trp in **4**, showed

good overlap as well, with both N−H bonds pointing inward. Despite the opposite alignment, (*R*)-**9** revealed a similar overlay (Figure 7B,D). While the aromatic moieties lined up in an opposite fashion, both the orientation of the suberic side chain and the amide N−H bond retained a good alignment. Interestingly, no segment of the isomers showed any overlap with the six-membered piperidine ring of apicidin A (**4**). The lack of selectivity between the enantiomers of **9** and HDACs can be due to the virtual similarity of the relative positions of pharmacophores (Figure 7C,D).

These pharmacophoric models highlight the role of **9** as a prototype for probing the cap region upon judicious embodiment of appropriate appendages, which might provide valuable structural, functional, and stereochemical insights into the design of new inhibitors.

Conclusion

On the basis of structural data on HDACs, we have reported the synthesis, biological activity, and pharmacophoric characterization of novel non-natural macrocyclic compounds as potential inhibitors of these enzymes. A small library of macrocyclic hydroxamic acids based on an analogue of **2** was prepared (compound **7**),[20] which displayed potent activity against 11 HDAC isoforms. A structure-based hypothesis guided the design of the novel macrocycles, in which the minimal functional requirements for HDAC activity were maintained. Critical amino acid residues highly conserved in the cap region of HDACs were taken into account in the design. The novel compounds were crafted following a uniform hierarchical approach relying on the combination of three building blocks, which were sequentially assembled by a phenolic Mitsunobu reaction or an amide coupling, followed by the formation of an anilide bond, and a ring closing metathesis reaction. All macrocycles were designed to contain a single stereogenic center, which led to enantiomers with an equivalent activity for the most promising hits. Macrocycles embedding two simple aromatic rings in the linker displayed a nanomolar activity profile against all isoforms [hydroxamic acids **9**, **10**, (*S*)-**34**, and (*S*)-**35**]. As expected for hydroxamic acid-containing HDAC inhibitors,[15,22] a preferential activity against HDAC6 in the nanomolar range was observed for all macrocycles. In particular, a relevant selectivity toward this isoform was detected within the group of diamide-based macrocycles (*R*)- and (*S*)-**36** and (*S*)-**37** (10−500-fold over the other HDACs). Given the role of HDAC6 in deacetylating α-tubulin and Hsp90, a high activity against this isozyme might be beneficial.[6] An excellent cytotoxic activity was also found for selected macrocycles against lung and colon cancer cell lines (H460 and HCT-116, respectively), often comparable or even superior to **2**.

Unnatural macrocyclic hydroxamic acids (*S*)- and (*R*)-**9**, together with the aza analogue (*S*)-**34**, emerged as the promising candidates from this study. Ligand-based analysis by rigid alignment of both enantiomers of **9** with the natural HDAC inhibitor apicidin A (**4**) led to the definition of general pharmacophoric models. Further refinement of these novel non-natural macrocyclic templates gives us hope for more potent and selective inhibitors of HDACs.

Experimental Section

Biological Assays. The purity of all tested compounds was assessed by HPLC and was ≥95%.

Cell Lines. HCT116 colon carcinoma cells and NCI-H460 non-small cell lung carcinoma cells were obtained from American Type Culture Collection. HCT-116 cells were grown in McCoy's 5A and NCI-H460 cells in RPMI-1640, both containing L-glutamine supplemented with 10% heat-inactivated fetal calf serum (FCS, Life Technologies) and 50 μg/mL gentamicin.

Cell Proliferation Assay. HCT-116 and NCI-H460 tumor cell lines were grown in a volume of 200 μL at approximately 10% confluency in 96-well multititer plates and were allowed to recover for an additional 24 h. Tumor cells were treated with either varying concentrations of drugs or solvent for 24 h. After the cells had been treated, the plates were washed to remove drug and incubated for 48 h. The fraction of cells surviving after compound treatment was determined using the SRB assay.[51] IC_{50} was defined as the drug concentration causing a 50% reduction in cell number compared with that of vehicle-treated cells and evaluated by the "ALLFIT" computer program by analyzing dose−response inhibition curves.

Histone Deacetylase Profiling. HDAC profiling was performed by Reaction Biology Corp. (Malvern, PA) against 11 isolated isoforms of human HDAC (HDAC1−11) in the presence of the fluorogenic tetrapeptide RHKKAc (p53 residues 379−382) as the substrate (10 μM). Isolated human HDACs were obtained by standard purification, with the exception of HDAC3, which was isolated in complex with NCOR2 and used as such. Inhibitors **1**, **2**, and dacinostat were used as reference compounds. Each compound was dissolved in DMSO (**1** and **2** at 10 μM), and sequentially diluted solutions were used for testing. IC_{50} values were calculated from the resulting sigmoidal dose−response inhibition slopes.

Conformational Analysis. Macrocycles were opened, and all the single bonds were allowed to rotate (0−180°) with the exception of hydroxamic acid and amide groups. Torsion checks were applied to amide and double bonds to preserve the *trans* and *cis* geometry, respectively. An implicit solvent model was used with the OPLS-2001 force field (Optimized Potentials for Liquid Simulations); all heavy atoms were used as a comparison, and 10000 steps of the Monte Carlo Multiple Minimum algorithm was used followed by 500 steps of Polak−Ribiere Conjugate Gradient (PRCG) minimization with a convergence threshold of 0.05. A multiple minimization was conducted with the aim of retaining mainly conformers with different macrocycle geometry, using 500 steps of Truncated Newton Conjugate Gradient (TNCG) minimization with a convergence threshold of 0.001. Conformers in the range of potential energy of 20 kJ/mol were retained, and a Boltzmann analysis was performed on the population minima. Calculations were performed using Macromodel version 9.6 (Schrödinger, LLC, New York, NY).

Macrocycles **8**−**10** and **34**−**37** revealed a preferential orientation of the *trans*-amide bond among the minimum conformers, which displayed the N−H bond pointing inside the cycle and eclipsing the adjacent aromatic ring (±20°). An opposite orientation could be observed when $\Delta E > 7$ kj/mol. In the case of **9**, the first four minimum energy conformers showed the aliphatic chain collapsed toward the macrocycle portion, interacting with the hydroxamic acid moiety via an intramolecular H-bond. The fifth conformer ($\Delta E = 4.684$ kj/mol, Boltzmann population of 6%) displayed a geometry very similar to that of the crystal structure of (*S*)-**32** ($rmsd_{heavy} = 0.31$ Å) and was chosen for docking analysis. Conformer populations of the other cyclic compounds were compared in an analogous way, and the macrocycle conformation closest to the one observed in the crystal structure of (*S*)-**32** was chosen as a starting conformation for docking studies.

Docking Procedures. A structure of HDAC8 cocrystallized with 4-(dimethylamino)-*N*-[7-(hydroxyamino)-7-oxoheptyl]-benzamide (MS-344) (PDB entry 1T67) was used for docking procedures. A conserved water molecule, H-bonded to His180 and interacting with the ligand, was retained. The protein was prepared according to the protein preparation protocol implemented in Maestro. Tyr100 dihedral χ_1 and χ_2 angles were

modified to increase the number of interactions with the macrocycles, in accord with the intrinsic mobility of this residue[7a] [see, for example, HDAC8 (PDB entry 2V5X)].

A structure of HDAC7 cocrystallized with **1** (PDB entry 3C10) was used for further modeling analysis. A conserved water molecule, H-bonded to His709 and interacting with **1**, was retained. The protein was prepared according to the protein preparation protocol.

Flexible docking was applied on each ligand, and a constraint was applied to allow the hydroxamic acid to correctly interact with Zn^{2+}. Ten poses were recorded; the pose with the best Emodel was used to compare score values. A further ligand minimization was performed within the active site, kept fixed, and out of it, and ΔE was calculated to evaluate the strain energy of the docking pose. All docking calculations were performed using Glide version 5.0 (Schrödinger, LLC). The binding site, for which the energy grid was calculated and stored, was defined with a cubic "bounding box" centered at the centroid of the respective cocrystallized ligands {4-(dimethylamino)-*N*-[7-(hydroxyamino)-7-oxoheptyl]benzamide in HDAC8 and **1** in HDAC7}, with an edge length of 12 Å in both proteins, and an "enclosing box" that would fit ligands up to lengths of 32 Å (HDAC8) and 28 Å (HDAC7).

Pharmacophore Model. The crystal structures of apicidin A (**4**) (Cambridge Crystallographic Data Centre, deposit no. CCDC 274844)[49] and (*S*)-**32** were modified by deletion of the Aoda and suberoyl hydroxamic acid tail, respectively. A rigid body alignment was conducted in MOE [Molecular Operating Enivroment (CCG, Montréal, QC)] using the default settings. The alignments were manually examined, and all alignments having different trajectories of the tail region were disregarded.

Acknowledgment. We thank Dr. Alexandra Furtos, Mr. Dalbir Sekong, and Dr. Sylvie Bilodeau of Centre Régional de Spectroscopie and of Service de RMN de l'Université de Montréal for their kind assistance. L.A. thanks the National Research Council of Italy (CNR), Institute of Biomolecular Chemistry, for a sabbatical leave. A postdoctoral grant from the Wenner-Gren Foundation, Sweden, is kindly acknowledged by A.L.

Supporting Information Available: Synthetic procedures; ^{1}H and ^{13}C NMR spectra of methyl esters (*R*/*S*)-**30a**−**c**, (*S*)-**32**, (*S*)-**33**, (*S*)-**39**, (*S*)-**47**, (*S*)-**54**, and (*S*)-**61** and hydroxamic acids (*R*/*S*)-**8a**−**c**, (*S*)-**9**, (*S*)-**10**, (*S*)-**34**, (*S*)-**35**, (*S*)-**36**, and (*S*)-**37**; further docking experiments (Figures SI1−SI5); and a CIF file and crystallographic data for (*S*)-**34**. This material is available free of charge via the Internet at http://pubs.acs.org.

References

(1) (a) Copeland, R. A.; Olhava, E. J.; Scott, M. P. Targeting Epigenetic Enzymes for Drug Discovery. *Curr. Opin. Chem. Biol.* **2010**, *14*, 505–510. (b) Peedicayl, J. Epigenetic Therapy: A New Development in Pharmacology. *Ind. J. Med. Res.* **2006**, *123*, 17–24. (c) Biel, M.; Wascholowski, V.; Giannis, A. Epigenetics—An Epicenter of Gene Regulation: Histones and Histone-Modifying Enzymes. *Angew. Chem., Int. Ed.* **2005**, *44*, 3186–3216.

(2) For recent reviews on HDAC role and inhibition, see: (a) Zhang, L.; Fang, H.; Xu, W. Strategies in Developing Promising Histone Deacetylase Inhibitors. *Med. Res. Rev.* **2009**, *30*, 585–602. (b) Paris, M.; Porcelloni, M.; Binaschi, M.; Fattori, D. Histone Deacetylase Inhibitors: From Bench to Clinic. *J. Med. Chem.* **2008**, *51*, 1505–1529. (c) Yang, X.-J.; Seto, E. HATs and HDACs: From Structure, Function and Regulation to Novel Strategies for Therapy and Prevention. *Oncogene* **2007**, *26*, 5310–5318. (d) Rodriquez, M.; Aquino, M.; Bruno, I.; De Martino, G.; Taddei, M.; Gomez-Paloma, L. Chemistry and Biology of Chromatin Remodeling Agents: State of Art and Future Perspectives of HDAC Inhibitors. *Curr. Med. Chem.* **2006**, *13*, 1119–1139. (e) Bolden, J. E.; Peart, M. J.; Johnstone, R. W. Anticancer Activities of Histone Deacetylase Inhibitors. *Nat. Rev. Drug Discovery* **2006**, *5*, 769–784. (f) Minucci, S.; Pelicci, P. G. Histone Deacetylase Inhibitors and the Promise of Epigenetic (and More) Treatments for Cancer. *Nat. Rev. Cancer* **2006**, *6*, 38–51. (g) Moradei, O.; Maroun, C. R.; Paquin, I.; Vaisburg, A. Histone Deacetylase Inhibitors: Latest Developments, Trends and Prospects. *Curr. Med. Chem.: Anti-Cancer Agents* **2005**, *5*, 529–560. (h) Mai, A.; Massa, S.; Rotili, D.; Cerbara, I.; Valente, S.; Pezzi, R.; Simeoni, S.; Ragno, R. Histone Deacetylation in Epigenetics: An Attractive Target for Anticancer Therapy. *Med. Res. Rev.* **2005**, *25*, 261–309. (i) Monneret, C. Histone Deacetylase Inhibitors. *Eur. J. Med. Chem.* **2005**, *40*, 1–13. (j) Dokmanovic, M.; Marks, P. A. Prospects: Histone Deacetylase Inhibitors. *J. Cell. Biochem.* **2005**, *96*, 293–304.

(3) Choudhary, C.; Kumar, C.; Gnad, F.; Nielsen, M. L.; Rehman, M.; Walther, T. C.; Olsen, J. V.; Mann, M. Lysine Acetylation Targets Protein Complexes and Co-Regulates Major Cellular Functions. *Science* **2009**, *325*, 834–840.

(4) Anzellotti, A. I.; Farrell, N. P. Zinc Metalloproteins as Medicinal Targets. *Chem. Soc. Rev.* **2008**, *37*, 1629–1651.

(5) Grozinger, C. M.; Schreiber, S. L. Deacetylase Enzymes: Biological Functions and the Use of Small-Molecule Inhibitors. *Chem. Biol.* **2002**, *9*, 3–16.

(6) For recent reviews on isoform-selective HDAC inhibitors, see: (a) Bertrand, P. Inside HDAC with HDAC Inhibitors. *Eur. J. Med. Chem.* **2010**, *45*, 2095–2116. (b) Balasubramanian, S.; Verner, E.; Buggy, J. J. Isoform-Specific Histone Deacetylase Inhibitors: The Next Step? *Cancer Lett.* **2009**, *280*, 211–221. (c) Witt, O.; Deubzer, H. E.; Milde, T.; Oehme, I. HDAC Family: What Are the Cancer Relevant Targets? *Cancer Lett.* **2009**, *277*, 8–21. (d) Khan, N.; Jeffers, M.; Kumar, S.; Hackett, C.; Boldog, F.; Khramtsov, N.; Qian, X.; Mills, E.; Berghs, S. C.; Carey, N.; Finn, P. W.; Collins, L. S.; Tumber, A.; Rithchie, J. W.; Jensen, P. B.; Lichenstein, H. S.; Sehested, M. Determination of the Class and Isoform Selectivity of Small-Molecule Histone Deacetylase Inhibitors. *Biochem. J.* **2008**, *409*, 581–589. (e) Bieliauskas, A. V.; Pflum, M. K. H. Isoform-Selective Histone Deacetylase Inhibitors. *Chem. Soc. Rev.* **2008**, *37*, 1402–1413. (f) Hildmann, C.; Wegener, D.; Riester, D.; Hempel, R.; Schober, A.; Merana, J.; Giurato, L.; Guccione, S.; Nielsen, T. K.; Ficner, R.; Schwienhorst, A. Substrate and Inhibitor Specificity of Class 1 and Class 2 Histone Deacetylase. *J. Biotechnol.* **2006**, *124*, 258–270.

(7) For the most relevant articles on HDAC structural biology, see the following. HDAC8: (a) Vannini, A.; Volpari, C.; Gallinari, P.; Jones, P.; Mattu, M.; Carfí, A.; De Francesco, R.; Steinkühler, C.; Di Marco, S. Substrate Binding to Histone Deacetylase as Shown by the Crystal Structure of the HDAC8-Substrate Complex. *EMBO Rep.* **2007**, *8*, 879–884. (b) Vannini, A.; Volpari, C.; Filocamo, G.; Casavola, E. C.; Brunetti, M.; Renzoni, D.; Chakravarty, P.; Paolini, C.; De Francesco, R.; Gallinari, P.; Steinkühler, C.; Di Marco, S. Crystal Structure of a Eukaryotic Zinc-Dependent Histone Deacetylase, Human HDAC8, Complexed with a Hydroxamic Acid Inhibitor. *Proc. Natl. Acad. Sci. U.S.A.* **2004**, *101*, 15064–15069. (c) Somoza, J. R.; Skene, R. J.; Katz, B. A.; Mol, C.; Ho, J. D.; Jennings, A. J.; Luong, C.; Arvai, A.; Buggy, J. J.; Chi, E.; Tang, J.; Sang, B.-C.; Verner, E.; Wynands, R.; Leahy, E. M.; Dougan, D. R.; Snell, G.; Navre, M.; Knuth, M. W.; Swanson, R. V.; McRee, D. E.; Tari, L. W. Structural Snapshots of Human HDAC8 Provide Insight into the Class I Histone Deacetylases. *Structure* **2004**, *12*, 1325–1334. HDAC7: (d) Schuetz, A.; Min, J.; Allali-Hassani, A.; Schapira, M.; Shuen, M.; Loppnau, P.; Mazitschek, R.; Kwiatkowski, N. P.; Lewis, T. A.; Maglathin, R. L.; McLean, T. H.; Bochkarev, A.; Plotnikov, A. N.; Vedadi, M.; Arrowsmith, C. H. Human HDAC7 Harbors a Class IIa Histone Deacetylase-Specific Zinc Binding Motif and Cryptic Deacetylase Activity. *J. Biol. Chem.* **2008**, *283*, 11355–11363. HDAC4: (e) Bottomley, M. J.; Lo Surdo, P.; Di Giovine, P.; Cirillo, A.; Scarpelli, R.; Ferrigno, F.; Jones, P.; Neddermann, P.; De Francesco, R.; Steinkühler, C.; Gallinari, P.; Carfí, A. Structural and Functional Analysis of the Human HDAC4 Catalytic Domain Reveals a Regulatory Structural Zinc-binding Domain. *J. Biol. Chem.* **2008**, *283*, 26694–26704. (f) Guo, L.; Han, A.; Bates, D. L.; Cao, J.; Chen, L. Crystal Structure of a Conserved N-Terminal Domain of Histone Deacetylase 4 Reveals Functional Insights into Glutamine Rich Domains. *Proc. Natl. Acad. Sci. U.S.A.* **2007**, *104*, 4297–4302. HDAC2: (g) Bressi, J. C.; Jennings, A. J.; Skene, R.; Wu, Y.; Melkus, R.; Jong, R. D.; O'Connell, S.; Grimshaw, C. E.; Navre, M.; Gangloff, A. R. Exploration of the HDAC2 Foot Pocket: Synthesis and SAR of Substituted N-(2-aminophenyl)benzamides. *Bioorg. Med. Chem. Lett.* **2010**, *20*, 3142–3145. HDLP (histone deacetylase-like protein): (h) Finnin, M. S.; Donigian, J. R.; Cohen, A.; Richon, V. M.; Rifkind, R. A.; Marks, P. A.; Breslow, R.; Pavletich, N. P. Structures of a Histone Deacetylase Homologue Bound to the TSA and SAHA Inhibitors. *Nature* **1999**, *401*, 188–193. See also: (i) http://www.actrec.gov.in/histone/infobase.htm.

(8) (a) Estiu, G.; West, N.; Mazitschek, R.; Greenberg, E.; Bradner, J. E.; Wiest, O. On the Inhibition of Histone Deacetylase 8. *Bioorg. Med. Chem.* **2010**, *18*, 4103–4110. (b) Ortore, G.; Di Colo, F.; Martinelli, A. Docking of Hydroxamic Acids into HDAC1 and

HDAC8: A Rationalization of Activity Trends and Selectivities. *J. Chem. Inf. Model.* **2009**, *49*, 2774–2785. (c) Estiu, G.; Greenberg, E.; Harrison, C. B.; Kwiatkowski, N. P.; Mazitschek, R.; Bradner, J. E.; Wiest, O. Structural Origin of Selectivity in Class II-Selective Histone Deacetylase Inhibitors. *J. Med. Chem.* **2008**, *51*, 2898–2906. (d) Wang, D.-F.; Helquist, P.; Wiech, N. L.; Wiest, O. Towards Selective Histone Deacetylase Inhibitor Design: Homology Modeling, Docking Studies, and Molecular Dynamics Simulations of Human Class I Histone Deacetylases. *J. Med. Chem.* **2005**, *48*, 6936–6947. (e) Wang, D.-F.; Wiest, O.; Helquist, P.; Lan-Hargest, H.-Y.; Wiech, N. L. On the Function of the 14 Å Long Internal Cavity of Histone Deacetylase-like Protein: Implication for the Design of Histone Deacetylase Inhibitors. *J. Med. Chem.* **2004**, *47*, 3409–3417.

(9) (a) Bradner, J. E.; West, N.; Grachan, M. L.; Greenberg, E. F.; Haggarty, S. J.; Warnow, T.; Mazitschek, R. Chemical Phylogenetics of Histone Deacetylases. *Nat. Chem. Biol.* **2010**, *6*, 238–243 and references cited therein . (b) Blackwell, L.; Norris, J.; Suto, C. M.; Janzen, W. P. The Use of Diversity Profiling to Characterize Chemical Modulators of the Histone Deacetylases. *Life Sci.* **2008**, *82*, 1050–1058. (c) Lahm, A.; Paolini, C.; Pallaoro, M.; Nardi, M. C.; Jones, P.; Nedderman, P.; Sambucini, S.; Bottomley, M. J.; Lo Surdo, P.; Carfí, A.; Koch, U.; De Francesco, R.; Steinkühler, C.; Gallinari, P. Unraveling the Hidden Catalytic Activity of Vertebrate Class IIa Histone Deacetylases. *Proc. Natl. Acad. Sci. U.S.A.* **2007**, *104*, 17335–17340. For a recent example of HDAC profiling in the development of a potent inhibitor, see: Arts, J.; King, P.; Mariën, A.; Floren, W.; Beliën, A.; Janssen, L.; Pilatte, I.; Roux, B.; Decrane, L.; Gilissen, R.; Hickson, I.; Vreys, V.; Cox, E.; Bol, K.; Talloen, W.; Goris, I.; Andries, L.; Du Jardin, M.; Janicot, M.; Page, M.; van Emelen, K.; Angibaud, P. JNJ-26481585, a Novel `Second Generation' Oral Histone Deacetylase Inhibitor, Shows Broad-Spectrum Preclinical Antitumoral Activity. *Clin. Cancer Res.* **2009**, *15*, 6841–6851.

(10) Relevant examples of selective HDAC inhibitors: (a) Ontoria, J. M.; Altamura, S.; Di Marco, A.; Ferrigno, F.; Laufer, R.; Muraglia, E.; Palumbi, M. C.; Rowley, M.; Scarpelli, R.; Schultz-Fademrecht, C.; Serafini, S.; Steinkühler, C.; Jones, P. Identification of Novel, Selective, and Stable Inhibitors of Class II Histone Deacetylases. Validation Studies of the Inhibition of the Enzymatic Activity of HDAC4 by Small Molecules as a Novel Approach for Cancer Therapy. *J. Med. Chem.* **2009**, *52*, 6782–6789. (b) Attenni, B.; Ontoria, J. M.; Cruz, J. C.; Rowley, M.; Schultz-Fademrecht, C.; Steinkühler, C.; Jones, P. Histone Deacetylase Inhibitors with a Primary Amide Zinc Binding Group Display Antitumor Activity in Xenograft Model. *Bioorg. Med. Chem. Lett.* **2009**, *19*, 3081–3084. (c) Schäfer, S.; Saunders, L.; Schlimme, S.; Valkov, V.; Wagner, J. M.; Kratz, F.; Sippl, W.; Verdin, E.; Jung, M. Pyridylalanine-Containing Hydroxamic Acids as Selective HDAC6 Inhibitors. *ChemMedChem* **2009**, *4*, 283–290. (d) Kozikowski, A. P.; Tapadar, S.; Luchini, D. N.; Kim, K. H.; Billadeau, D. D. Use of the Nitrile Oxide Cycloaddition (NOC) Reaction for Molecular Probe Generation: A New Class of Enzyme Selective Histone Deacetylase Inhibitors (HDACIs) Showing Picomolar Activity at HDAC6. *J. Med. Chem.* **2008**, *51*, 4370–4373. (e) Zhou, N.; Moradei, O.; Raeppel, S.; Leit, S.; Frechette, S.; Gaudette, F.; Paquin, I.; Bernstein, N.; Bouchain, G.; Vaisburg, A.; Jin, Z.; Gillespie, J.; Wang, J.; Fournel, M.; Yan, P. T.; Trachy-Bourget, M.-C.; Kalita, A.; Lu, A.; Rahil, J.; MacLeod, A. R.; Li, Z.; Besterman, J. M.; Delorme, D. Discovery of N-(2-Aminophenyl)-4-[(4-pyridin-3-ylpyrimidin-2-ylamino)methyl]benzamide (MGCD0103), an Orally Active Histone Deacetylase Inhibitor. *J. Med. Chem.* **2008**, *51*, 4072–4075. (f) Suzuki, T.; Kouketsu, A.; Itoh, Y.; Hisakawa, S.; Maeda, S.; Yoshida, M.; Nakagawa, H.; Miyata, N. Highly Potent and Selective Histone Deacetylase 6 Inhibitor Designed Based on a Small-Molecular Substrate. *J. Med. Chem.* **2006**, *49*, 4809–4812. (g) Jones, P.; Altamura, S.; Chakravarty, P. K.; Checchetti, O.; De Francesco, R.; Gallinari, P.; Ingenito, R.; Meinke, P. T.; Petrocchi, A.; Rowley, M.; Scarpelli, R.; Serafini, S.; Steinkühler, C. A Series of Novel, Potent, and Selective Histone Deacetylase Inhibitors. *Bioorg. Med. Chem. Lett.* **2006**, *16*, 5948–5952. (h) Haggarty, S. J.; Koeller, K. M.; Wong, J. C.; Grozinger, C. M.; Schreiber, S. L. Domain-Selective Small-Molecule Inhibitor of Histone Deacetylase 6 (HDAC6)-Mediated Tubulin Deacetylation. *Proc. Natl. Acad. Sci. U.S.A.* **2003**, *100*, 4389–4394. (i) Mai, A.; Massa, S.; Pezzi, R.; Rotili, D.; Loidl, P.; Brosch, G. Discovery of (Aryloxopropenyl)-pyrrolyl Hydroxyamides as Selective Inhibitors of Class IIa Histone Deacetylase Homologue HD1-A. *J. Med. Chem.* **2003**, *46*, 4826–4829.

(11) Isolation and activity: (a) Tsuji, N.; Kobayashi, M.; Nagashima, K.; Wakisaka, Y.; Koizumi, K. A New Antifungal Antibiotic, Trichostatin. *J. Antibiot.* **1976**, *29*, 1–6. (b) Yoshida, M.; Kijima, M.; Akita, M.; Beppu, T. Potent and Specific Inhibition of Mammalian Histone Deacetylase Both In Vivo and In Vitro by Trichostatin A. *J. Biol. Chem.* **1990**, *265*, 17174–17179. Synthesis: (c) Mori, K.; Koseki, K. Synthesis of Trichostatin A, a Potent Differentiation Inducer of Friend Leukemic Cells, and Its Antipode. *Tetrahedron* **1998**, *44*, 6013–6020.

(12) (a) Grant, S.; Easley, C.; Kirkpatrick, P. Vorinostat. *Nat. Rev. Drug Discovery* **2007**, *6*, 21–22. (b) Marks, P. A.; Breslow, R. Dimethyl Sulfoxide to Vorinostat: Development of This Histone Deacetylase Inhibitor as an Anticancer Drug. *Nat. Biotechnol.* **2007**, *25*, 84–90. (c) Gediya, L. K.; Chopra, P.; Purushottamachar, P.; Maheshwari, N.; Njar, V. C. O. A New Simple and High-Yield Synthesis of Suberoylanilide Hydroxamic Acid and Its Inhibitory Effect Alone or in Combination with Retinoids on Proliferation of Human Prostate Cancer Cells. *J. Med. Chem.* **2005**, *48*, 5047–5051. (d) Huang, L.; Pardee, A. B. Suberoylanilide Hydroxamic Acid as a Potential Therapeutic Agent for Human Breast Cancer Treatment. *Mol. Med.* **2000**, *6*, 849–866. (e) Butler, L. M.; Agus, D. B.; Scher, H. I.; Higgins, B.; Rose, A.; Cordon-Cardo, C.; Thaler, H. T.; Rifkind, R. A.; Marks, P. A.; Richon, V. M.; LaQuaglia, M. P. Suberoylanilide Hydroxamic Acid, an Inhibitor of Histone Deacetylase, Suppresses the Growth of Prostate Cancer Cells in Vitro and in Vivo. *Cancer Res.* **2000**, *60*, 5165–5170.

(13) Examples of natural macrocyclic inhibitors. Trapoxin: (a) Kijima, M.; Yoshida, M.; Sugita, K.; Horinouchi, S.; Beppu, T. Trapoxin, an Antitumor Cyclic Tetrapeptide, Is an Irreversible Inhibitor of Mammalian Histone Deacetylase. *J. Biol. Chem.* **1993**, *268*, 22429–22435. Apicidin: (b) Singh, S. B.; Zink, D. L.; Liesch, J. M.; Mosley, R. T.; Dombrowski, A. W.; Bills, G. F.; Darkin-Rattray, S. J.; Schmatz, D. M.; Goetz, M. A. Structure and Chemistry of Apicidins, a Class of Novel Cyclic Tetrapeptides without a Terminal α-Keto Epoxide as Inhibitors of Histone Deacetylase with Potent Antiprotozoal Activities. *J. Org. Chem.* **2002**, *67*, 815–825. FK228: (c) Konstantinopoulos, P. A.; Vandoros, G. P.; Papavassiliou, A. G. FK288 (Depsipeptide): A HDAC Inhibitor with Pleiotropic Antitumor Activities. *Cancer Chemother. Pharmacol.* **2006**, *58*, 711–715. Spiruchostatins: (d) Masuoka, Y.; Nagai, A.; Shin-Ya, K.; Furihata, K.; Nagai, K.; Suzuki, K.-I.; Hayakawa, Y.; Seto, H. Spiruchostatins A and B, Novel Gene Expression-Enhancing Substances Produced by Pseudomonas sp. *Tetrahedron Lett.* **2001**, *42*, 41–44. Azumamides: (e) Nakao, Y.; Yoshida, S.; Matsunaga, S.; Shindoh, N.; Terada, Y.; Nagai, K.; Yamashita, J. K.; Ganesan, A.; van Soest, R. W. M.; Fusetani, N. Azumamides A-E: Histone Deacetylase Inhibitory Cyclic Tetrapeptides from the Marine Sponge Mycale izuensis. *Angew. Chem., Int. Ed.* **2006**, *45*, 7553–7557. FR23522: (f) Xie, W.; Zou, B.; Pei, D.; Ma, D. Total Synthesis of Cyclic Tetrapeptide FR235222, a Potent Immunosuppressant that Inhibits Mammalian Histone Deacetylase. *Org. Lett.* **2005**, *7*, 2775–2777. Largazole: (g) Bowers, A.; West, N.; Taunton, J.; Schreiber, S. L.; Bradner, J. E.; Williams, R. M. Total Synthesis and Biological Mode of Action of Largazole: A Potent Class I Histone Deacetylase Inhibitor. *J. Am. Chem. Soc.* **2008**, *130*, 11219–11222. (h) Ying, Y.; Taori, K.; Kim, H.; Hong, J.; Luesch, H. Total Synthesis and Molecular Target of Largazole, a Histone Deacetylase Inhibitor. *J. Am. Chem. Soc.* **2008**, *130*, 8455–8459.

(14) For reviews on alternative zinc-binding groups in the design of HDAC inhibitors, see: (a) Suzuki, T.; Naoki, M. Rational Design of Non-Hydroxamate Histone Deacetylase Inhibitors. *Mini-Rev. Med. Chem.* **2006**, *6*, 515–526. (b) Suzuki, T.; Miyata, N. Non-hydroxamate Histone Deacetylase Inhibitors. *Curr. Med. Chem.* **2005**, *12*, 2867–2880. (c) Vanommeslaege, K.; Loverix, S.; Geerlings, P.; Tourwé, D. DFT-Based Ranking of Zinc-Binding Groups in Histone Deacetylase Inhibitors. *Bioorg. Med. Chem.* **2005**, *13*, 6070–6082. For an application, see: (d) Hanessian, S.; Vinci, V.; Auzzas, L.; Marzi, M.; Giannini, G. Exploring alternative Zn-binding groups in the design of HDAC inhibitors: Squaric Acid, N-Hydroxyurea, and Oxazoline Analogues of SAHA. *Bioorg. Med. Chem. Lett.* **2006**, *16*, 4784–4787.

(15) Furumai, R.; Komatsu, Y.; Nishino, N.; Khochbin, S.; Yoshida, M.; Korinouchi, S. Potent Histone Deacetylase Inhibitors Built from Trichostatin A and Cyclic Tetrapeptide Antibiotics Including Trapoxin. *Proc. Natl. Acad. Sci. U.S.A.* **2001**, *98*, 87–92.

(16) Sternson, S. M.; Wong, J. C.; Grozinger, C. M.; Schreiber, S. L. Synthesis of 7200 Small Molecules Based on a Substructural Analysis of the Histone Deacetylase Inhibitors Trichostatin and Trapoxin. *Org. Lett.* **2001**, *3*, 4239–4242.

(17) For examples of synthetic macrocyclic peptides, see the following. Apicidin analogues: (a) Olsen, C. A.; Ghadiri, M. R. Discovery of Potent and Selective Histone Deacetylase Inhibitors via Focused Combinatorial Libraries of Cyclic α3β-Tetrapeptides. *J. Med. Chem.* **2009**, *52*, 7836–7846. (b) Montero, A.; Beierle, J. M.; Olsen, C. A.; Ghadiri, M. R. Design, Synthesis, Biological Evaluation, and Structural Characterization of Potent Histone Deacetylase Inhibitors Based on Cyclic α/β-Tetrapeptide Architectures. *J. Am. Chem. Soc.* **2009**, *131*, 3033–3041. (c) Deshmukh, P. H.; Schulz-Fademrecht, C.; Procopiou, P. A.; Vigushin, D. A.; Coombes, R. C.; Barrett, A. G. M. Ring-Closing Metathesis in the Synthesis of Biologically Active Peptidomimetics of Apicidin A. *Adv. Synth. Catal.* **2007**, *349*, 175–183. FK228 analogues, Largazole: (d) Bowers, A. A.; Greshock, T. J.; West, N.; Estiu, G.; Schreiber, S. L.; Wiest, O.; Williams, R. M.; Bradner, J. E. Synthesis and Conformation-Activity Relationships of

the Peptide Isosteres of FK228 and Largazole. *J. Am. Chem. Soc.* **2009**, *131*, 2900–2905. (e) Di Maro, S.; Pong, R.-C.; Hsieh, J.-T.; Ahn, J.-M. Efficient Solid-Phase Synthesis of FK228 Analogues as Potent Antitumoral Agents. *J. Med. Chem.* **2008**, *51*, 6639–6641. (f) Yurek-George, A.; Cecil, A. R. L.; Mo, A. H. K.; Wen, S.; Habens, F.; Maeda, S.; Yoshida, M.; Packham, G.; Ganesan, A. The First Biologically Active Synthetic Analogue of FK228, the Depsipeptide Histone Deacetylase Inhibitor. *J. Med. Chem.* **2007**, *50*, 5720–5726. Azumamides analogues: (g) Wen, S.; Carey, K. L.; Nakao, Y.; Fusetani, N.; Packham, G.; Ganesan, A. Total Synthesis of Azumamide A and Azumamide E, Evaluation as Histone Deacetylase Inhibitors, and Design of a More Potent Analogue. *Org. Lett.* **2007**, *9*, 1105–1108. (h) Maulucci, N.; Chini, M. G.; Di Micco, S.; Izzo, I.; Cafaro, E.; Russo, A.; Gallinari, P.; Paolini, C.; Nardi, M. C.; Casapullo, A.; Riccio, R.; Bifulco, G.; De Riccardis, F. Molecular Insight into Azumamide E Histone Deacetylases Inhibitory Activity. *J. Am. Chem. Soc.* **2007**, *129*, 3007–3012. Cyclostellettamine analogues: (i) Pérez-Balado, C.; Nebbioso, A.; Rodríguez-Graña, P.; Minichiello, A.; Miceli, M.; Altucci, L.; de Lera, Á. R. Bispyridinium Dienes: Histone Deacetylase Inhibitors with Selective Activities. *J. Med. Chem.* **2007**, *50*, 2497–2505.

(18) For a recent highlight on the potential of natural and non-natural macrocycles for drug discovery, see: Drigger, E. M.; Hale, S. P.; Lee, J.; Terret, N. K. The Exploration of Macrocycles for Drug Discovery: An Underexploited Structural Class. *Nat. Rev. Drug Discovery* **2008**, *7*, 608–624.

(19) Non-natural macrocyclic HDAC inhibitors: (a) Mwakwari, S. C.; Guerrant, W.; Patil, V.; Khan, S. I.; Tekwani, B. L.; Gurard-Levin, Z. A.; Mrksich, M.; Oyelere, A. K. Non-Peptide Macrocyclic Histone Deacetylase Inhibitors Derived from Tricyclic Ketolide Skeleton. *J. Med. Chem.* **2010**, *53*, 6100–6111 and references cited therein. (b) Liu, T.; Kapustin, G.; Etzkorn, F. A. Design and Synthesis of a Potent Histone Deacetylase Inhibitor. *J. Med. Chem.* **2007**, *50*, 2003–2006. (c) Curtin, M. L.; Garland, R. B.; Heyman, H. R.; Frey, R. R.; Michaelides, M. R.; Li, J.; Lori, J. P.; Glaser, K. B.; Marcotte, P. A.; Davidsen, S. K. Succinimide Hydroxamic Acids as Potent Inhibitors of Histone Deacetylase (HDAC). *Bioorg. Med. Chem. Lett.* **2002**, *12*, 2919–2923. See also: (d) Pérez-Balado, C.; Nebbioso, A.; Rodríguez-Graña, P.; Minichiello, A.; Miceli, M. Bispyridinium Dienes: Histone Deacetylase Inhibitors with Selective Activities. *J. Med. Chem.* **2007**, *50*, 2497–2505.

(20) (a) Hanessian, S.; Auzzas, L.; Larsson, A.; Zhang, J.; Giannini, G.; Gallo, G.; Ciacci, A.; Cabri, W. Vorinostat-like Molecules as Structural, Stereochemical and Pharmacological Tools. *ACS Med. Chem. Lett.* **2010**, *1*, 70–74. (b) Hanessian, S.; Auzzas, L.; Giannini, G.; Marzi, M.; Cabri, W.; Barbarino, M.; Vesci, L.; Pisano, C. ω-Alkoxy Analogues of SAHA (Vorinostat) as Inhibitors of HDAC: A Study of Chain-Length and Stereochemical Dependence. *Bioorg. Med. Chem. Lett.* **2007**, *17*, 6261–6265.

(21) In addition, the binding was stabilized by interactions between the amide bond of the *R* and *S* isomers with a conserved water molecule and with an Asp residue (Asp101 in HDAC8), respectively. Furthermore, a H-bond between the methoxy group of the *S* isomer and Lys33 was observed stabilizing the complex in HDAC8. The Lys residue is present only in this HDAC isoform.

(22) Only a hydroxamic acid head can conceivably ensure this premise, at least in principle. For example, certain ketone-based inhibitors were found to be discriminating depending on their chirality (see ref 7a).

(23) These residues are conserved among the class I HDAC1, HDAC2, HDAC3, and HDAC8 isoforms and the class II HDAC4 isoform (see ref 7).

(24) Giannini, G.; Hanessian, S.; Auzzas, L.; Cabri, W.; Battistuzzi, G.; Vesci, L.; Pisano, C. Synthesis and Evaluation of In Vitro Activity of Novel SAHA-like Derivatives as Histone Deacetylase Inhibitors. 2009 American Association Cancer Research Annual Meeting, April 18−22, 2009, Denver, CO, Abstract 622.

(25) (a) Hughes, D. L. Progress in the Mitsunobu Reaction. A review. *Org. Prep. Proced. Int.* **1996**, *28*, 127–164. (b) Hughes, D. L. The Mitsunobu Reaction. *Org. React.* **1992**, *42*, 335–356. (c) Mitsunobu, O. The Use of Diethyl Azodicarboxylate and Triphenylphosphine in Synthesis and Transformation of Natural Products. *Synthesis* **1981**, 1–28.

(26) Aniline **21a** was prepared according to a published procedure: Beckwith, A. L. J.; Gara, W. B. Phosphorylated Sugars. Part XV. Syntheses of 3-Deoxy-D-erythro- and 3-Deoxy-D-threo-hexulosonic Acid 6-(Dihydrogen Phosphates). *J. Chem. Soc., Perkin Trans. 1* **1975**, 593–600.

(27) Zhao, H.; Thurkauf, A. A Practical and Convenient Synthesis of Methyl 5-Formyl-3-Methoxybenzoate. *Synth. Commun.* **2001**, *31*, 1921–1926.

(28) Zimmerman, H. E.; Jones, G., II Exploratory and Mechanistic Organic Photochemistry. XLVII. Photochemistry of a Cyclohexadienone Structurally Incapable of Rearrangement. *J. Am. Chem. Soc.* **1970**, *92*, 2753–2761.

(29) Leading references on olefin metathesis: (a) *Handbook of Metathesis*; Grubbs, R. H., Ed.; Wiley-VCH: Weinheim, Germany, 2003; Vols. 1−3. (b) Grubbs, R. H. Olefin Metathesis. *Tetrahedron* **2004**, *60*, 7117–7140. (c) Deiters, A.; Martin, S. F. Synthesis of Oxygen- and Nitrogen-Containing Heterocycles by Ring-Closing Metathesis. *Chem. Rev.* **2004**, *104*, 2199–2238. For an excellent review on the RCM with nitrogen-containing compounds, see: (d) Phillips, A. J.; Abell, A. D. Ring-Closing Metathesis of Nitrogen-Containing Compounds: Applications to Heterocycles, Alkaloids, and Peptidomimetics. *Aldrichimica Acta* **1999**, *32*, 75–89.

(30) Scholl, M.; Ding, S.; Lee, C. W.; Grubbs, R. H. Synthesis and Activity of a New Generation of Ruthenium-Based Olefin Metathesis Catalysts Coordinated with 1,3-Dimesityl-4,5-dihydroimidazol-2-ylidene Ligands. *Org. Lett.* **1999**, *1*, 953–956.

(31) Li, H.; Jiang, X.; Ye, Y.-H.; Fan, C.; Romoff, T.; Goodman, M. 3-(Diethoxyphosphoryloxy)-1,2,3- benzotriazin-4(3H)-one (DEPBT): A New Coupling Reagent with Remarkable Resistance to Racemization. *Org. Lett.* **1999**, *1*, 91–93.

(32) Kingsbury, J. S.; Harrity, J. P. A.; Bonitatebus, P. J., Jr.; Hoveyda, A. H. A Recyclable Ru-Based Metathesis Catalyst. *J. Am. Chem. Soc.* **1999**, *121*, 791–799.

(33) For the use of $^{n}BuNH_2$ for preventing *O*-benzyl cleavage, see: Czech, B. P.; Bartsch, R. A. Effect of Amines on *O*-Benzyl Group Hydrogenolysis. *J. Org. Chem.* **1984**, *49*, 4076–4078.

(34) (a) Catley, L.; Weisberg, E.; Tai, Y. T.; Atadja, P.; Remiszewski, S.; Hideshima, T.; Mitsiades, N.; Shringarpure, R.; LeBlanc, R.; Chauhan, D.; Munshi, N. C.; Schlossman, R.; Richardsone, P.; Griffin, J.; Anderson, K. C. NVP-LAQ824 Is a Potent Novel Histone Deacetylase Inhibitor with Significant Activity Against Multiple Myeloma. *Blood* **2003**, *102*, 2615–2622. (b) Remiszewski, S. W. The Discovery of NVP-LAQ824: From Concept to Clinic. *Curr. Med. Chem.* **2003**, *10*, 2393–2402.

(35) Screening was performed by Reaction Biology Corp., Malvern, PA.

(36) The slight difference in activity between the two isomers of **9** against class II HDACs [$IC_{50(S/R)}$ = 0.08−0.28] can be justified by a preferential interaction between the methoxyphenyl ring of the *S* isomer and loop 1, which contains a conserved His-Pro motif in these isozymes (Figure SI3 of the Supporting Information).

(37) An equivalent stabilization was predicted for the *R* isomer.

(38) Docking of (*S*)-**35** to HDAC8 accounted for interactions similar to those observed with (*S*)-**9**. An extra stabilization was detected between Phe208 and the anilido ring of (*S*)-**35**.

(39) In particular, the *S* isomer of **37** was predicted to gain a better stabilization than its enantiomeric counterpart, thanks to a favorable interaction between the indole motif and Tyr100 (see Figure SI5 of the Supporting Information).

(40) Quite interestingly, no significant *N*-Boc deprotection of the starting material was detected. The conditions described for this metathesis reaction proved to be nonreproducible in further trials, leading to an even lower yield of macrocycle (*S*)-**39**. Other catalysts (Grubbs' first or second generation) under various conditions (solvents, temperature, additives) were unsuccessful.

(41) Thompson, A. S.; Humphrey, G. R.; DeMarco, A. M.; Mathre, D. J.; Grabowski, E. J. J. Direct Conversion of Activated Alcohols to Azides Using Diphenyl Phosphorazidate. A Practical Alternative to Mitsunobu Conditions. *J. Org. Chem.* **1993**, *58*, 5886–5888.

(42) Gololobov, Y. G.; Zhmurova, I. N.; Kasukhin, L. F. Sixty Years of Staudinger Reaction. *Tetrahedron* **1981**, *37*, 437–472.

(43) Upadhyaya, D. J.; Barge, A.; Stefania, R.; Cravotto, G. Efficient, Solventless *N*-Boc Protection of Amines Carried Out at Room Temperature Using Sulfamic Acid as Recyclable Catalyst. *Tetrahedron Lett.* **2007**, *48*, 8318–8322.

(44) The formation of homocoupling side products and a significant decomposition of the starting material were observed.

(45) Abarbri, M.; Thibonnet, J.; Bérillon, L.; Dehmel, F.; Rottländer, M.; Knochel, P. Preparation of New Polyfunctional Magnesiated Heterocycles Using a Chlorine-, Bromine-, or Iodine-Magnesium Exchange. *J. Org. Chem.* **2000**, *65*, 4618–4634.

(46) (a) Hanessian, S.; Giroux, S.; Larsson, A. Efficient Allyl to Propenyl Isomerization in Functionally Diverse Compounds with a Thermally Modified Grubbs Second-Generation Catalyst. *Org. Lett.* **2006**, *8*, 5481–5484. (b) Beinhoff, M.; Weigel, W.; Rettig, W.; Bruedgam, I.; Hartl, H.; Schlueter, A. D. Phenylene Alkylene Dendrons with Site-Specific Incorporated Fluorescent Pyrene Probes. *J. Org. Chem.* **2005**, *70*, 6583–6591.

(47) Trost, B. M.; Arndt, H. C.; Strege, P. E.; Verhoeven, T. R. Desulfonylation of aryl alkyl sulfones. *Tetrahedron Lett.* **1976**, *17*, 3477−3478.

(48) With the exception of HDAC8 (Tyr100) and HDAC10 (Phe90), Phe566 in HDAC6 corresponds to nonaromatic and polar amino acids in the other isoforms (F566E in HDAC1 and HDAC2, F566D in HDAC3, F566T in HDAC7, and F566S in HDAC4, HDAC5, and HDAC9) (see ref 7e).

(49) Apicidin X-ray: Cambridge Crystallographic Data Centre, deposit CCDC 274844: Kranz, M.; Murray, P. J.; Taylor, S.; Upton, R. J.; Clegg, W.; Elsegood, M. R. J. Solution, Solid Phase and Computational Structures of Apicidin and Its Backbone-Reduced Analogs. *J. Pept. Sci.* **2006**, *12*, 383–388.
(50) Horne, W. S.; Olsen, C. A.; Beierle, J. M.; Montero, A.; Ghadiri, M. R. Probing the Bioactive Conformation of an Archetypal Natural Product HDAC Inhibitor with Conformationally Homogeneous Triazole-Modified Cyclic Tetrapeptides. *Angew. Chem., Int. Ed.* **2009**, *48*, 1–7.
(51) Skehan, P.; Storeng, R.; Scudiero, D.; Monks, A.; McMahon, J.; Vistica, D.; Warren, J. T.; Bokesch, H.; Kenney, S.; Boyd, M. R. New Colorimetric Citotoxycity Assay for Anticancer-drug Screening. *J. Natl. Cancer Inst.* **1990**, *82*, 1107–1112.